JOURNAL OF DIFFERENTIAL EQUATIONS 58, 104–156 (1985)

Tranversality of the Invariant Manifolds Associated to the Lyapunov Family of Periodic Orbits near L_2 in the Restricted Three-Body Problem

JAUME LLIBRE AND REGINA MARTÍNEZ

Secció de Matemàtiques, Facultat de Ciències, Universitat Autònoma de Barcelona, Barcelona, Spain

AND

CARLES SIMÓ

Facultat de Matemàtiques, Universitat de Barcelona, Barcelona, Spain

Received July 7, 1983; revised January 19, 1984

The restricted three-body problem is considered for values of the Jacobi constant C near the value C_2 associated to the Euler critical point L_2. A Lyapunov family of periodic orbits near L_2, the so-called family (c), is born for $C = C_2$ and exists for values of C less than C_2. These periodic orbits are hyperbolic. The corresponding invariant manifolds meet transversally along homoclinic orbits. In this paper the variation of the transversality is analyzed as a function of the Jacobi constant C and of the mass parameter μ. Asymptotical expressions of the invariant manifolds for $C \lesssim C_2$ and $\mu \gtrsim 0$ are found. Several numerical experiments provide accurate information for the manifolds and a good agreement is found with the asymptotical expressions. Symbolic dynamic techniques are used to show the existence of a large class of motions. In particular the existence of orbits passing in a random way (in a given sense) from the region near one primary to the region near the other is proved.

1. INTRODUCTION AND STATEMENT OF THE RESULTS

Let S and J be two bodies called Sun and Jupiter, of masses $m_S = 1 - \mu$ and $m_J = \mu$, $\mu \in (0, 1)$, respectively, describing circular orbits. The center of masses is placed at the origin. In a rotating frame (synodical coordinates) the equations of motion of a massless particle P under the gravitational action of S and J are

$$\begin{aligned} \ddot{x} - 2\dot{y} &= \Omega_x, \\ \ddot{y} + 2\dot{x} &= \Omega_y, \end{aligned} \tag{1.1}$$

0022-0396/85 $3.00

where

$$\Omega = \Omega(x, y) = \frac{1-\mu}{r_1} + \frac{\mu}{r_2} + \frac{1}{2}(x^2 + y^2) + \frac{1}{2}\mu(1-\mu)$$

and $r_1^2 = (x-\mu)^2 + y^2$, $r_2^2 = (x+1-\mu)^2 + y^2$ (see [15]). Equations (1.1) are called the equations of the restricted three-body problem (RTBP) and they have a first integral (Jacobi integral) given by

$$F(x, y, \dot{x}, \dot{y}) = -(\dot{x}^2 + \dot{y}^2) + 2\Omega(x, y).$$

It is well known that the system (1.1) has five equilibrium points, three on the axis $y = 0$ (Euler points) called L_1, L_2, L_3 and two equilateral points (Lagrange points, forming an equilateral triangle with S and J) called L_4, L_5 (see Fig. 1.1). The value of F at the point L_i will be denoted by C_i. For all μ, $C_4 = C_5 = 3$ are less than C_1, C_2, C_3. For $\mu \in (0, \frac{1}{2})$ one has $C_3 < C_1 < C_2$. We keep the name L_i for the equilibrium points in the phase space as well as in the position plane.

We can restrict ourselves to study the flow on the hypersurface

$$M(\mu, C) = \{(x, y, \dot{x}, \dot{y}) \in \mathbb{R}^4 | F(x, y, \dot{x}, \dot{y}) = C\}.$$

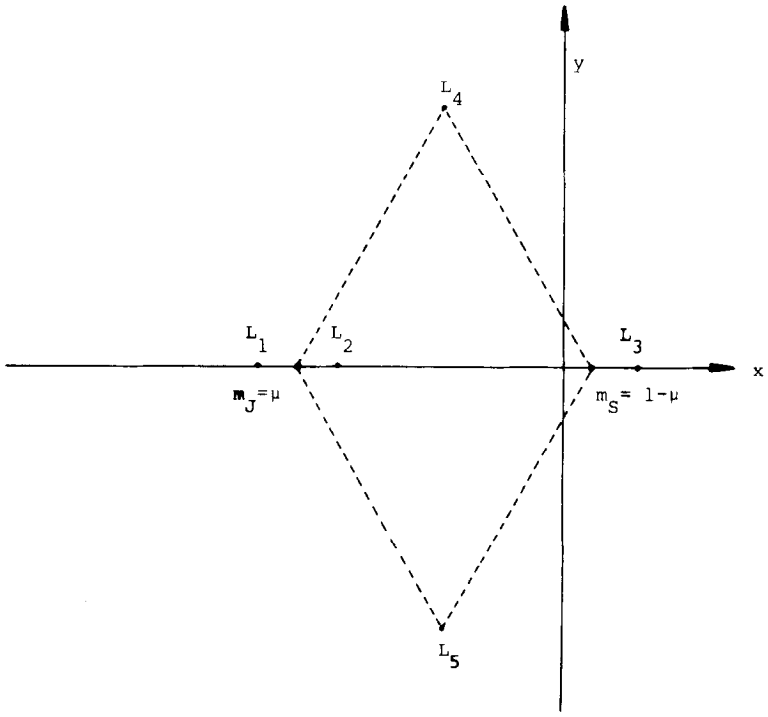

FIG. 1.1. Equilibrium points of the restricted three-body problem.

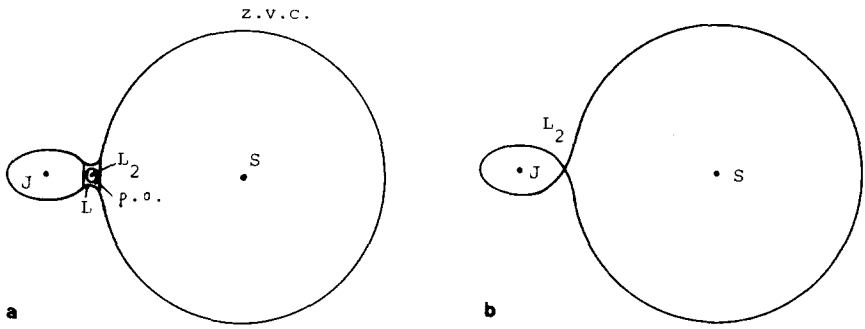

FIG. 1.2. Bounded Hill's region: (a) for $C \lesssim C_2$; (b) for $C = C_2$.

The projection of $M(\mu, C)$ on the position plane is the so-called Hill's region

$$R(\mu, C) = \{(x, y) \in \mathbb{R}^2 | \Omega(x, y) \geqslant C/2\}.$$

The boundary of $R(\mu, C)$ is the zero velocity curve (z.v.c.), empty if C is less than C_4. For $C \in (C_1, C_2)$ the Hill's region has two components, one of them bounded, that we call $R_b(\mu, C)$ (Fig. 1.2a). The component of $M(\mu, C)$ projecting on $R_b(\mu, C)$ will be called $M_b(\mu, C)$. Note that $M_b(\mu, C)$ is unbounded in the phase space due to the fact that the velocity of P tends to infinity when P tends to S or J. Binary collisions can be regularized but, as this is of no interest for the present study, we don not care about such singularities.

The main purpose of this paper is the study of the motion of P in $M_b(\mu, C)$. For $C = C_2$, $M_b(\mu, C) - \{L_2\}$ has two components whose boundaries meet at L_2 (see Fig. 1.2b). These two components will be called region S and region J depending on the fact that they contain the point S or the point J. For $C \lesssim C_2$ we can take two segments on $R_b(\mu, C)$ joining points in the z.v.c. (see Fig. 1.2a) such that they give a partition of $R_b(\mu, C)$ in three components. One of the components contains the projection of the periodic orbit (p.o.) near L_2. We call this component region L. The other two contain the points S and J and they will be called again region S and region J, respectively. As before we keep the same name, region S, L or J for the sets in the phase space whose projections are the regions S, L or J, respectively, in the position plane.

Near L_2 and for values of $C \lesssim C_2$ there is a family of hyperbolic periodic orbits (parameterized by C) which receives the name of family (c) in the classical terminology (see [15]). When $C \uparrow C_2$ the periodic orbit (p.o.) tends to L_2. The eigenvalues of the linearized equations associated to (1.1) at L_2 are of the form $\pm\lambda$, $\pm i\nu$, $\lambda, \nu \in \mathbb{R}_+$. There are one-dimensional invariant stable, $W^s_{L_2}$, and unstable, $W^u_{L_2}$, manifolds associated to L_2 (see Section 2 and [8]).

In a similar way the p.o. of the (c) family have two-dimensional invariant manifolds $W^s_{\text{p.o.}}$, $W^u_{\text{p.o.}}$, locally diffeomorphic to cylinders. We recall that a homoclinic orbit (h.o.) related to an equilibrium point E or to a periodic orbit $\bar{E}$ is an orbit such that tends to E (or $\bar{E}$) for $t \to \pm\infty$. Therefore it is on the stable and unstable invariant manifolds of the related object (E or $\bar{E}$). A homoclinic orbit is called transversal if at some point of the orbit the tangent spaces to the stable and unstable manifolds at that point span the full tangent space to $M(\mu, C)$ at the same point. If W^u, W^s are one-dimensional, the existence of a h.o. implies that both manifolds coincide with the h.o.

As is known Eq. (1.1) have the following symmetry:

$$S: (x, y, \dot{x}, \dot{y}, t) \to (x, -y, -\dot{x}, \dot{y}, -t). \tag{1.2}$$

Therefore, if we know the unstable manifold of L_2 or of the p.o. (which is a symmetrical p.o.) the corresponding stable manifold is obtained through the use of the stated symmetry.

In Section 4 we prove the following analytical results.

THEOREM A. *For μ sufficiently small the branch $W^{u,S}_{L_2}$ of $W^u_{L_2}$ contained in the S region has a projection on $R_h(\mu, C)$ given by (see Fig. 1.3a).*

$$d = \mu^{1/3}(\tfrac{2}{3} N(\infty) - 3^{1/6} + M(\infty)\cos t + o(1)),$$

$$\alpha = -\pi + \mu^{1/3}(N(\infty)\, t + 2M(\infty)\sin t + o(1)),$$

where d is the distance to the z.v.c., α the angular coordinate, $N(\infty)$ and $M(\infty)$ are constants (see Section 4) and the expressions remain true out of a given neighborhood of L_2. The parameter t means the physical time from a suitable origin. The terms $o(1)$ tend to zero when μ does and they are uniform in t for $t = O(\mu^{-1/3})$.

In particular the first intersection with the x axis is orthogonal to that axis, giving a h.o. for a sequence of values of μ which has the following asymptotical expression:

$$\mu_k = \frac{1}{N(\infty)^3 k^3}(1 + o(1)).$$

THEOREM B. *If μ and $\Delta C = C_2 - C$ are sufficiently small the branch $W^{u,S}_{\text{p.o.}}$ of $W^u_{\text{p.o.}}$ contained initially in the S region intersects $y = 0$ for $x > 0$ in a curve diffeomorphic to a circle given by*

$$x = x_w + \mu^{1/3} M(1 - \cos M_f)$$
$$+ \mu^{2/3} \left\{ -\frac{2MN}{3}(1 - \cos M_f) + M^2 \sin^2 M_f - \frac{2}{9} N\bar{\alpha} - \frac{M}{3}\bar{\alpha} \cos M_f \right.$$
$$- \bar{\beta}^{1/2}(N + 2M \cos \tau)^{-1}(2M + N \cos M_f)(K_1 \cos \tau \cos \sigma$$
$$\left. - K_2 \sin \tau \sin \sigma) \right\} + O(\mu),$$

$$\dot{x} = \sin M_f \left[\mu^{1/3} M + \mu^{2/3} \left\{ \frac{MN}{3} + 2M^2 \cos M_f + \frac{M}{3}\bar{\alpha} \right.\right.$$
$$\left.\left. + \bar{\beta}^{1/2} N(N + 2M \cos \tau)^{-1}(K_1 \cos \tau \cos \sigma - K_2 \sin \tau \sin \sigma) \right\} \right] + O(\mu),$$

where x_w, M, N, τ, K_1, K_2 *are suitable constants,* $\bar{\alpha}$ *measures the distance from* μ *to some* μ_k *given by Theorem* A, $\bar{\beta} = \Delta C/\mu^{4/3}$, M_f *is obtained implicitly from*

$$\left(\frac{1}{3} N\bar{\alpha} + \bar{\beta}^{1/2} 3M(N + 2M \cos \tau)^{-1}(K_1 \cos \tau \cos \sigma - K_2 \sin \tau \sin \sigma) \right) \frac{\pi}{N}$$
$$+ NM_f + 2M \sin M_f = o(1)$$

and σ, *ranging from* 0 *to* 2π, *is the parameter of the curve* (*see Section* 4 *for a detailed discussion about the shape of this curve and the geometrical meaning of the constants, Fig.* 1.3b *and figures of Section* 5). *In particular, for points in the* (μ, C) *plane such that there is a* μ_k *of Theorem* A *for which* $\Delta C > L\mu_k^{4/3}(\mu - \mu_k)^2$ *holds* (*where* L *is a constant depending on the previous ones*) *there are symmetrical transversal homoclinic orbits.*

In order to test the formulas given above several numerical experiments have been performed. First we have obtained values μ_k of the mass parameter μ for which the invariant manifolds of L_2 are homoclinic orbits

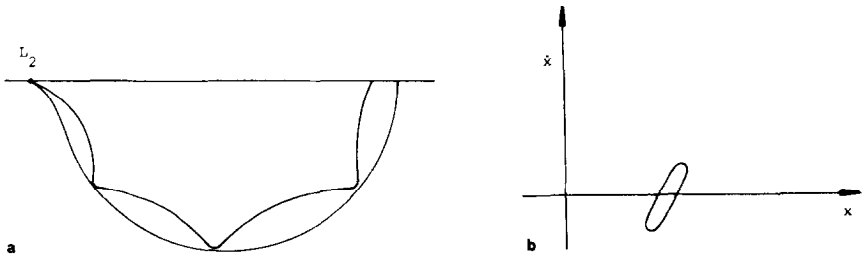

FIG. 1.3. (a) Projection of the right branch of $W^u_{L_2}$ on the (x, y) plane. (b) First section of the right branch of $W^u_{\text{p.o.}}$ with $y = 0$ in the region $x > 0$.

which intersect only one time $y=0$ in the region $x>0$. Between two consecutive values of μ such that $W^u_{L_2}$ crosses for the first time the x axis orthogonally, the slope of the projection when crossing that axis has one extremum. Values of the masses for which those extrema are attained are given. This provides information about the shape of $W^u_{L_2}$.

In a similar way we study numerically the invariant manifolds for the periodic orbit with $C \lesssim C_2$. Several intersections for different values of ΔC and μ are given. An adequate selection of values of μ and C for which non-transversal h.o. exist gives the boundary of the region of plane (μ, C) referred to in Theorem B.

As a last series of computations the case of the neighbourhood of the small primary is studied. This is a perturbation of the Hill's problem [15]. We present numerical results for the invariant manifolds in the Hill's problem and for small perturbations (μ sufficiently small).

In Section 6 we prove the existence of some shift as a subsystem of the RTBP. The alphabet is in this case the set of all integers with absolute value bounded from below. The main result in this section is the following one (we present here a simplified version).

THEOREM C. *Consider a region S or J and a doubly infinite sequence of integers $(\ldots, m_{-2}, m_{-1}, m_0, m_1, m_2, \ldots)$ where $|m_j| > m = m(\mu, C)$, $\forall j \in \mathbb{Z}$. Then there exist initial conditions (unique in a neighbourhood of certain h.o.) such that the orbit corresponding to those conditions enters the L region and leaves it going to the initial region or to the opposite according to whether m_0 is positive or not. The number of integer revolutions of the projection of the orbit on $R_b(\mu, C)$ around L_2 while the orbit remains in L is $|m_0|$. After that the same process begins again with m_1 in the place of m_0, m_2 in the place of m_1, etc. For negative time a similar behavior is described being m_{-1}, m_{-2},... the associated integers. For this orbit the number of integer revolutions of the massless body around the Sun or Jupiter when the orbit is in the S or J region, respectively, is a constant depending on the region and on the selected homoclinic orbits.*

In fact, in Section 6 we present an abstract version of this result from which Theorem C follows. Other consequences and different motions (some of them can be seen as a compactification of the motions of Theorem C including asymptotic and doubly asymptotic motions) are given.

The existence of motions in restricted problems like the described was first proved by Sitnikov [13]. The theorems of embedding of the shift based on an alphabet of two elements near homoclinic points of diffeomorphisms started with the paper of Smale [14]. A generalization of the results of Sitnikov showing how to embed the shift on infinite elements in two-dimensional diffeomorphisms was given by Alekseev [1]. A simplified

geometrical version of this type of statements was offered by Moser [12]. The present paper is an extension of a previous work that can be found in [10]. Through the paper free use is made of several important results contained in McGehee's Ph.D. thesis [9], mainly concerned with the nonlinear behaviour near L_2 for small enough μ and ΔC.

We note that quasirandom motions whose existence is proved in Theorem C can be confined in a bounded region of the phase space. This is a situation different from the one we encounter in other three-body problems, for instance, in the Sitnikov problem, in the outer region of the circular restricted problem for C large enough [6] and in the collinear general three-body problem [7]. In these works a crucial role is played by a periodic orbit "at the infinity."

2. The Flow near the Equilibrium Point

Using the Moser–Lyapunov theorem [11] the flow near L_2 was described by Conley in [3] and [4]. We briefly recall the results.

Let P be an equilibrium point of a hamiltonian with two degrees of freedom. We suppose that the eigenvalues of the linearized field at P are $\pm\lambda$, $\pm\nu i$, λ, $\nu \in \mathbb{R}_+$. Therefore, moving P to the origin, the analytical hamiltonian H can be written in the form

$$H(x, y, \dot{x}, \dot{y}) = \lambda x\dot{x} + \tfrac{1}{2}\nu(y^2 + \dot{y}^2) + O_3(x, y, \dot{x}, \dot{y}). \tag{2.1}$$

If we only take into account the linear terms the functions $x\dot{x}$, $y^2 + \dot{y}^2$ are first integrals. Using the Moser–Lyapunov theorem, Conley [3] showed that in a neighbourhood of P the flow of the hamiltonian (2.1) is analytically conjugated to the flow of the linearized equations.

In fact, a convenient change of coordinates transforms (2.1) into the hamiltonian

$$K(\xi, \eta, \zeta, \bar{\zeta}) = \lambda\xi\eta + \frac{\nu}{2}|\zeta|^2 + O_2(\xi\eta, |\zeta|^2) \tag{2.2}$$

having $\xi\eta = x\dot{x} + O_3(x, y, \dot{x}, \dot{y})$ and $|\zeta|^2 = y^2 + \dot{y}^2 + O_3(x, y, \dot{x}, \dot{y})$ as first integrals.

For the points L_1, L_2, L_3 the linear part fulfills the hypotheses. Therefore the flow near those points can be described in the following way. We consider a fixed value of C, $C < C_2$, C_2-C small. The region L in the phase space is analytically diffeomorphic to $[0, 1] \times S^2$. The boundaries are two spheres l_1, l_2 projecting on $R_b(\mu, C)$ as a segment joining two points of the z.v.c. (Fig. 1.2a). The sphere l_1 belongs to the boundary of the S region (in fact it is exactly the boundary). In a similar way l_2 is the boundary of the

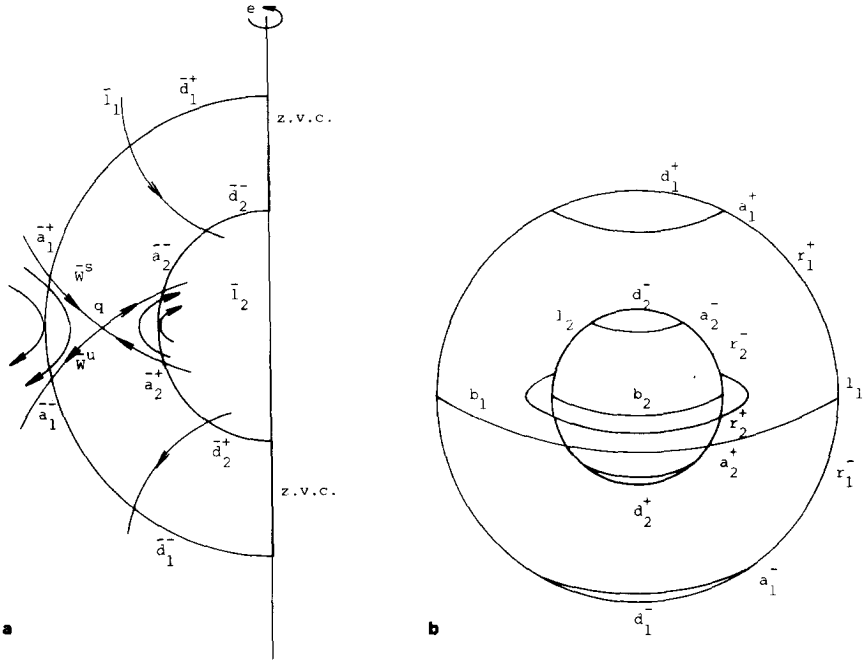

FIG. 2.1. The flow in the L region.

J region. These two spheres can be obtained by rotation of two half circles $\bar{l}_1$, $\bar{l}_2$ around a suitable axis e (see Fig. 2.1a). The region L is obtained by the rotation of the points bounded by $\bar{l}_1, \bar{l}_2, e$. In L there is a hyperbolic p.o. given in the picture by the point q and the associated invariant manifolds are obtained from the arcs $\bar{W}^{u,s}$. We note that if the hamiltonian is of the form $H(x, y, \dot{x}, \dot{y}) = \frac{1}{2}(\dot{x}^2 + \dot{y}^2) + V(x, y)$ the p.o. near the point P on a given level of energy reaches the z.v.c. in two points [5]. Therefore the projection of this p.o. on the position plane is an arc travelled twice. This is not true for the RTBP (due to the Coriolis force), where the projection is a simple closed curve.

The manifold l_1 can be split into two open hemispheres l_1^+, l_1^- where the flow enters or leaves L. The flow is tangent to the boundary circle b_1 of l_1^+ and l_1^-. Similar hemispheres l_2^+, l_2^- and circle b_2 can be found on l_2.

The manifolds W^s, W^u intersect the spheres l_1, l_2 in four circles $a_1^+, a_2^+, a_1^-, a_2^-$. Using the variables of (2.2) those circles are given by $|\zeta|^2 = r^*$ where r^* is a suitable constant (see [3]). The circles a_1^+, a_1^- (resp. a_2^+, a_2^-) determine on l_1 (resp. l_2) a couple of spherical caps, d_1^+, d_1^- (resp. d_2^+, d_2^-) corresponding to transit orbits going from S to J or vice versa (see Fig. 2.1b). There are orbits going from S to L and returning to S. They enter L through a spherical zone r_1^+ whose boundary $a_1^+ \cup b_1$ and leave it

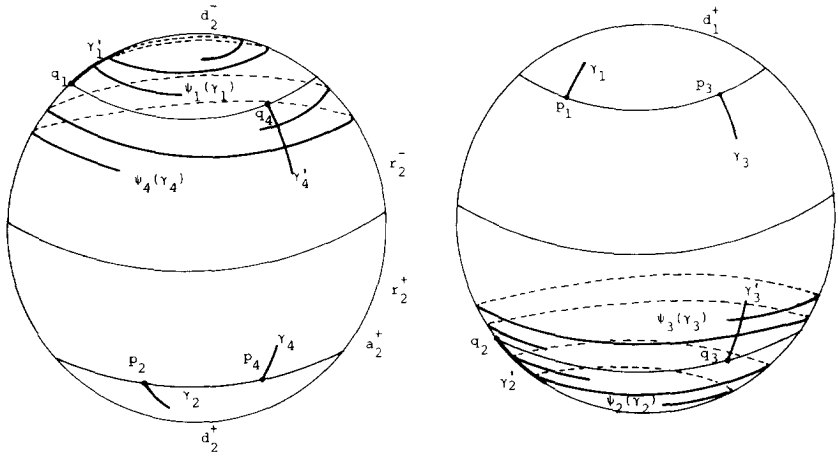

FIG. 2.2. Spiraling of the images of arcs γ_i, $i = 1, 2, 3, 4$, under the suitable Poincaré maps.

through r_1^- whose boundary is $a_1^- \cup b_1$. Symmetrical zones r_2^+, r_2^- exist in l_2.

The behavior of the flow in L is obtained by adding some spiraling to the arrows given in Fig. 2.1a.

On the level $C = C_2$ the p.o. degenerates into the point L_2. The invariant manifolds $W_{L_2}^{u,s}$ of the p.o. become one-dimensional (and therefore they are orbits of the system). Local expressions for these manifolds were given by Lukjanov [8].

As the flow is transversal to $l_{1,2}^{\pm}$ we can define the maps

$$\psi_1 : d_1^+ \to d_2^-, \qquad \psi_2 : d_2^+ \to d_1^-,$$
$$\psi_3 : r_1^+ \to r_1^-, \qquad \psi_4 : r_2^+ \to r_2^-,$$

obtained following the flow in L. The four mappings are diffeomorphisms.

Let γ_i be an arc in the domain of ψ_i with ending point P_i on $a_1^+, a_2^+, a_1^+, a_2^+$ for $i = 1, ,2, 3, 4$, respectively. Let γ_i' be an arbitrary arc in the image of ψ_i such that one of its ending points Q_i is on $a_2^-, a_1^-, a_1^-, a_2^-$ for $i = 1, 2, 3, 4$, resp. Then $\psi_i \gamma_i$ is an arc spiraling towards $a_2^-, a_1^-, a_1^-, a_2^-$, resp. and cutting γ_i' on an infinity of points in any neighbourhood of Q_i (Fig. 2.2 and see [3]).

3. A Suitable Poincaré Map for the Problem

In the plane μ, C we consider, for μ_0 sufficiently small, an open neighbourhood of the curve $C_2(\mu)$ for $\mu \in (0, \mu_0)$, which does not intersect

$C_1(\mu)$. A suitable choice of the boundaries of L (see McGehee [9]) allows us to show two important facts. In the region S there is an invariant two-dimensional torus T such that separates the Sun from the L region. His projection on $R_b(\mu, C)$ is the annulus given in Fig. 3.1. Let N be the submanifold of $M_b(\mu, C)$ whose boundary is $T \cup l_1$. Then there exists an increasing function θ: $N \to \mathbb{R}$ where θ is a longitudinal angular coordinate. The region of the (μ, C) plane where this result is true will be called McGehee's region from now on. The proof of this last result is based on a careful study of the perturbation of the line $C = C_2(\mu)$ near $\mu = 0$, $C = C_2(0)$. We call $\bar{N}$ the projection of N on the Hill's region.

We cut the flow by the plane $y = 0$. The branch of the manifold $W^u_{\text{p.o.}}$ which enters the S region cuts the plane $y = 0$ on the part $\bar{N}_{\text{far}}$ of $\bar{N}$ opposite to L with respect to the Sun in a curve analytically diffeomorphic to a circle (at least when we are, say, in McGehee's region). We call this intersection the first cut of $W^{u,S}_{\text{p.o.}}$ (Sun) with $y = 0$. Note that in order to define the first cut we exclude a neighbourhood of l_1 in the S region. Some arcs of this curve produce successive intersections without leaving the S region. The q^{th} of these intersections of $W^{u,S}_{\text{p.o.}}$ with $y = 0$ will be called $\Gamma^{u,S}_q$. In a similar way we call $\Gamma^{s,S}_p$ the corresponding pth intersection with $y = 0$ of the Sun's branch of $W^s_{\text{p.o.}}$.

In the J region we can define arcs $\Gamma^{u,J}_{q'}$, $\Gamma^{s,J}_{p'}$ in an analogous way. Note that no analog of the increasing θ theorem of McGehee is available now. For the cases $p' = 1$ and $q' = 1$ we exclude a neighbourhood of l_2 as we did before with l_1.

Let us suppose that $W^{u,S}_{\text{p.o.}}$ does not coincide with $W^{s,S}_{\text{p.o.}}$ and $W^{u,J}_{\text{p.o.}}$ does not coincide with $W^{s,J}_{\text{p.o.}}$. For all positive values of μ, C-C_2 sufficiently small the first part of the hypothesis is analytically shown to be true in Section 4.

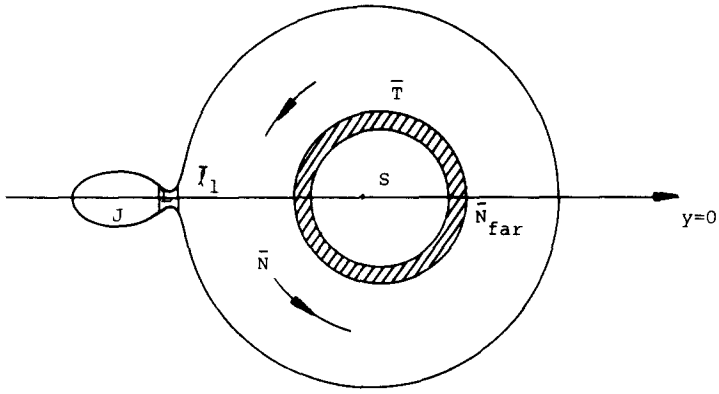

FIG. 3.1. Projection of the global picture of the flow in N.

Numerical experiments give us regions of the (μ, C) plane where the second part of the hypothesis is also true (see Section 5).

The existence of arcs belonging to $\Gamma_q^{u,S}$, $\Gamma_p^{s,S}$, $\Gamma_{q'}^{u,J}$, $\Gamma_{p'}^{s,J}$ for all natural values of q, p, q', p' is guaranteed by spiraling and a measure preservation argument on l_1, l_2 using canonical variables. A point in $y=0$ belonging to $\Gamma_q^{u,S} \cap \Gamma_p^{s,S}$ (if not empty) will be called a (q, p)-homoclinic point (h.p.). Of course, every (q, p)-h.p. originates a $(\bar{q}, \bar{p})$-h.p. under forward or backwards flow if $\bar{q}+\bar{p}=q+p$. The existence of (q, p)-homoclinic points for some q and p is shown in [3, 4]. In Sections 4 and 5 we show the existence of (1, 1)-transversal h.p. for some values of μ, C and where they are located. A point in the J region is called (q', p')-homoclinic if it belongs to $\Gamma_{q'}^{u,J} \cap \Gamma_{p'}^{s,J}$. Due to the fact that in this region the problem is a perturbation of the Hill's problem (nonintegrable) there are no analytic arguments proving the existence of some concrete (q', p')-h.p. However, the Conley reasoning using preservation of area applies and numerically it will be seen the existence of (6, 6)-h.p. for some μ, C.

Some subarcs of $\Gamma_q^{u,S}$ can produce no intersection with $y=0$ in the S region for positive time without leaving S. However, they can cross to the J region and there we get image arcs on $y=0$. The intersection of these images with arcs of the $\Gamma_{p'}^{s,J}$ type will not be considered here. The fact that some of these intersections are not empty can be shown using spiraling and measure preservation on l_1, l_2.

Let r be a small positive quantity. We define A, B, C, D, E, F, G and H as the set of points of d_1^+, r_1^+, r_1^-, d_1^-, d_2^-, r_2^-, r_2^+ and d_2^+, respectively, such that $||\zeta|^2 - r^*| < r$ (see Section 2 and Fig. 3.2). If r is small enough the flow is transversal to the surfaces just defined. Orbits entering L through

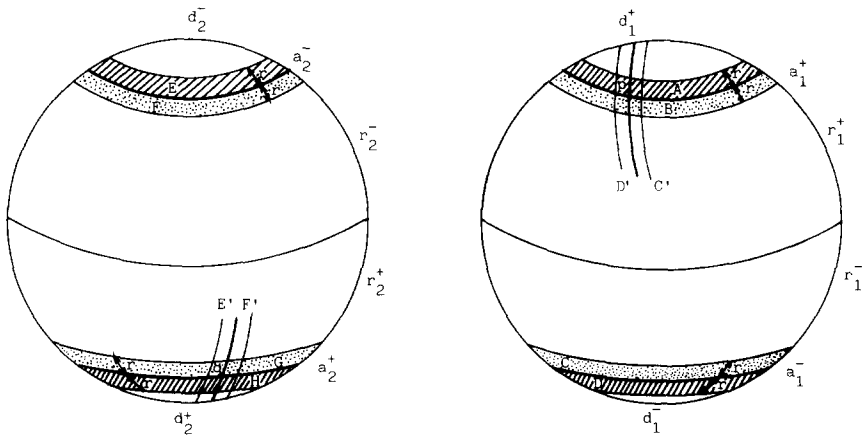

FIG. 3.2. Strips near invariant manifolds on the spheres l_1, l_2.

A, B, G, H leave it through E, C, F, D, respectively, because $|\zeta|^2$ is a first integral in L. Therefore the diffeomorphisms ψ_1 send A, H, B and G into E, D, C and F for $i = 1, 2, 3$ and 4, respectively.

Let us suppose that there exist $(1, 1)$-transversal h.o. in the Sun and Jupiter regions. A similar study can be done for (p, q)-h.o. in the S region and (p', q')-h.o. in the Jupiter region. Let $p \in a_1^+$ (resp. $q \in a_2^+$) be a point of a transversal h.o. of $(1, 1)$ type in the Sun region (resp. in the Jupiter region). Let D' and C' (resp. E' and F') be the first images of D and C (resp. E and F) by the flow outside L in l_1 (resp. l_2). The maps sending D, C, E, F into D', C', E', F' are diffeomorphisms. In a neighbourhood of p (resp. q) the qualitative picture of D' and C' (resp. E' and F') is shown in Fig. 3.2 provided r is sufficiently small.

Let U_S (resp. U_J) be the sets diffeomorphic to $(A \cup B) \cap (D' \cup C')$ (resp. $(G \cup H) \cap (E' \cup F')$) defined following the flow backwards up to the first crossing with the surface $y = 0$. Let $U = U_S \cup U_J$. We define f: $U \to U$ in the following way: To each point $x \in U$ we assign the corresponding first intersection point of the orbit passing through x with U, if it exists. Note that f is not defined in all the points of U. The map f is a "singular cross section" in the sense of Devaney [5]. We loosely refer to U as

$$U = [(A \cup B) \cap (D' \cup C')] \cup [(G \cup H) \cap (E' \cup F')]$$

even being U contained in the surface $y = 0$.

Now we state a property of the Poincaré map f, just defined, that will be used in Section 6. Let X be the intersection of the manifolds $M_b(\mu, C)$ and $y = 0$. In X we can choose $(x, \dot{x})$ as coordinates since $y = 0$ and $\dot{y}$ can be obtained from the Jacobi integral. We call again S the symmetry defined in (1.2) when we restrict it to X.

LEMMA 3.1. $f^{-1} = S^{-1} \circ f \circ S$.

4. ANALYTICAL RESULTS

In this section the main objectives are to obtain expressions of $W^u_{L_2}$ as a function of μ and of $W^u_{\text{p.o.}}$ as a function of μ and ΔC. Then the proofs of Theorems A and B will be easy corollaries of this two computations. First of all we need to recall some results about Hill's problem. This problem studies the behavior near the small mass of the RTBP in the limit when $\mu \to 0$. To get the limit equations we shift the origin to the small mass and scale before letting μ go to zero through $(x, y) \to ((x + 1 - \mu)\mu^{-1/3}, y\mu^{-1/3})$. By substitution on (1.1) we get

$$\begin{aligned}\ddot{x}-2\dot{y} &= 3x - x(x^2+y^2)^{-3/2} + \mu^{1/3}(\mu-1)(r_1^2+r_1+1)\,r_1^{-3} \\ &\quad \times (r_1+1)^{-1}(x^2+y^2) \\ &\quad + x(-2+(1-\mu)\,r_1^{-3}(2r_1^2+r_1+1)(r_1+1)^{-1}) \\ &= 3x - x(x^2+y^2)^{-3/2} + \mu^{1/3}(6x^2+3y^2/2) + O(\mu^{2/3}), \qquad (4.1) \\ \ddot{y}+2\dot{x} &= -y(x^2+y^2)^{-3/2} + y(1-(1-\mu)\,r_1^{-3}) \\ &= -y(x^2+y^2)^{-3/2} - \mu^{1/3}(3xy) + O(\mu^{2/3}),\end{aligned}$$

where $r_1^2 = (x^2+y^2)\,\mu^{2/3} - 2x\mu^{1/3} + 1$. Hill's problem is obtained by putting $\mu = 0$ in (4.1), i.e.,

$$\begin{aligned}\ddot{x}-2\dot{y} &= 3x - x(x^2+y^2)^{-3/2} = \Omega_x^H(x, y), \\ \ddot{y}+2\dot{x} &= -y(x^2+y^2)^{-3/2} \quad = \Omega_y^H(x, y),\end{aligned} \qquad (4.2)$$

where $\Omega^H(x, y) = \frac{1}{2}(3x^2 + 2(x^2+y^2)^{-1/2})$.

System (4.2) has a Jacobi first integral given by

$$C^H = 2\Omega^H(x, y) - \dot{x}^2 - \dot{y}^2.$$

From (4.1) it is clear that near the small mass μ in suitable coordinates the RTBP can be seen as a perturbation of order $\mu^{1/3}$ of the Hill problem.

For the Hill problem he equilibrium points L_1, L_2 are given by $(\mp 3^{-1/3}, 0)$ and the related value of C^H is $3^{4/3}$. The zero velocity curve for this value of C^H is given by

$$y = \pm(\tfrac{4}{9}(3^{1/3} - x^2)^{-2} - x^2)^{1/2}, \qquad |x| < 3^{1/6}.$$

For $|x| = 3^{1/6}$ the curve has two vertical asymptotes (see Fig. 4.1).

The critical points are saddle-centers. The eigenvalues are the roots of $\lambda^4 - 2\lambda^2 - 27 = 0$. The eigenvalue associated to the unstable manifold $W_{L_2}^{u,H}$ is $\lambda = (1 + 2\cdot 7^{1/2})^{1/2}$, and the angle α between the tangent at L_2 to the projection of $W_{L_2}^{u,H}$ on the (x, y) plane and the x axis is given by $\tan\alpha = -2\lambda(\lambda^2+3)^{-1}$ (see Fig. 4.1).

A straightforward computation shows that a local expression for $W_{L_2}^{u,H}$ is

$$\begin{aligned}x &= 3^{-1/3} + s + (14\lambda^2 - 459)\,3^{7/3}s^2(1296 + 906\lambda^2)^{-1} + O(s^3), \\ y &= (\lambda^2 - 9)\,s(2\lambda)^{-1} + (81 - 13\lambda^2)\,3^{7/3}s^2[2\lambda(24\lambda^2 + 405)]^{-1} + O(s^3),\end{aligned}$$

where $s = \exp(\lambda t)$. Note that an equivalent expression can be obtained from [8] after a suitable scaling of variables and a shift of the origin.

In [9, pp. 48–52] it is proved that the qualitative picture for the flow on the right of L_2 until some value x_o of x strictly smaller than $3^{1/6}$ is the same

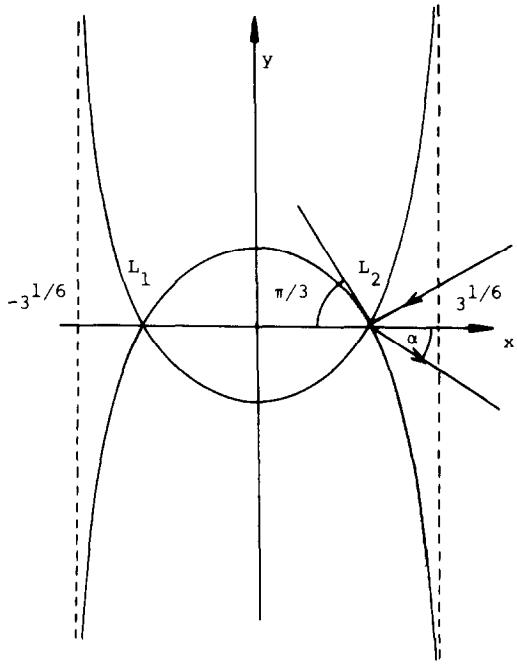

FIG. 4.1. Zero velocity curves for the Hill's problem and $C^H = C_{L_2}$.

as the one given by the linearized flow (see Section 2). Therefore $W^{u,H}_{L_2}$ crosses $x = x_o$ going to the right. By continuity with respect to μ this is also true for the related unstable manifold $W^{u,\mu}_{L_2}$ of the RTBP for μ sufficiently small.

Following [9] we introduce some notation. Let $a = x + iy$, $b = (\dot{x} - y) + i(\dot{y} + x) \in \mathbb{C}$. Then system (1.1) can be written in hamiltonian form $\dot{a} = H_{\bar{b}}$, $\dot{b} = -H_{\bar{a}}$ where $\bar{a}$ denotes the conjugate of a and $H(a, b, \mu)$ is given by

$$H(a, b, \mu) = |b|^2 + i(\bar{a}b - a\bar{b}) - 2V(a, \mu),$$

$V(a,\mu)$ being equal to $(1-\mu)|a+\mu|^{-1} + \mu|a+\mu-1|^{-1}$.

The Levi–Civita transformation $a = 2z^2$, $b = wz^{-1}$ allows us to introduce the variable $\xi = w + ihz$, where $h = (2V(a, \mu) - |b|^2)^{1/2}$. Let $\theta = \text{Arg } \xi$. In the RTBP let us suppose that μ is sufficiently small and the Jacobi constant C is equal or slightly smaller than C_2.

As the RTBP far from the equilibrium points and far from the primary m_J for μ sufficiently small can be seen as a perturbation of the synodical two-body problem (S2BP) there are invariant tori in the region S (see Section 3) which are not far from the z.v.c. The region S can be defined (see [9, pp. 18, 32]) as the points of $M_b(\mu, C)$ such that $x > x_{L_2} + \mu^{1/3}k$ where k can be taken slightly smaller than $3^{1/6}$.

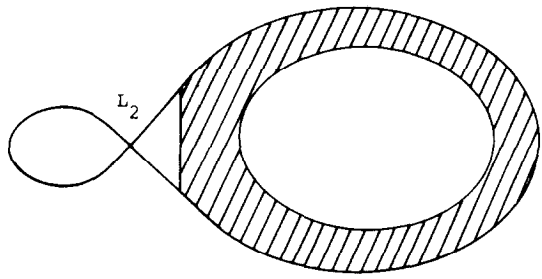

FIG. 4.2. The shaded area is the projection of N.

Let N be a region projecting on the position plane in a small annulus whose outer boundary is the z.v.c. and the line $x = x_{L_2} + \mu^{1/3}k$, and the inner boundary coincides with the outer boundary of the projection of some of the invariant tori just mentioned. In [9, Theorem 1] it is proved that in N the argument θ is strictly increasing along orbits while the orbit remains in N (see Fig. 4.2 and Section 3).

While one orbit remains in N its position vector a has modulus $|a|$ near 1. Therefore $|(\dot{x}, \dot{y})|$ is small because (x, y) is near the z.v.c.

For $\mu = 0$ an easy computation shows that

$$2^{1/2}\xi = i(x+iy)^{1/2}[(2(x^2+y^2)^{-1/2} - ((\dot{x}-y)^2 + (\dot{y}+x)^2))^{1/2} + (x^2+y^2)^{1/2}] + (\dot{x}+i\dot{y})(x-iy)^{1/2},$$

and in N, ξ is continuous with respect to μ. The first term on the right is a complex with modulus near 2 and the second one near zero. Therefore the argument of $x+iy$ is near $2\theta - \pi$. By continuity this is also true for the RTBP if μ is small enough. This result does not imply that the argument of the position vector with respect to the origin is always increasing. Small loops can be present as it happens in the S2BP (see Fig. 4.3).

Let $\bar{k}$ be such that $\bar{k} \cdot \mu^{1/3} < \frac{1}{2}$. Then an orbit entering in N through the 2-sphere projecting on the line $x = x_{L_2} + \mu^{1/3}k$ crosses the line $y = -\bar{k}\mu^{1/3}$. Scaling the variables as in (4.1) this means that the orbit crosses $y = -\bar{k}$. From (4.1) it follows that the piece of $W^{u,\mu}_{L_2}$ in scaled variables between L_2 and $y = -\bar{k}$ for some constant $\bar{k}$ and μ small enough converges to the

FIG. 4.3. Possible behavior for the position vector of the orbit in the S2BP near the z.v.c.

similar piece of the manifold $W^{u,H}_{L_2}$ (this is locally true in a neighborhood of L_2 and after we have a perturbation $O(\mu^{1/3})$ acting on a finite time).

Hence $W^{u,H}_{L_2}$ crosses the line $y = -\bar{k}$, for any fixed value of $\bar{k}$, going down forwards.

Now we study the behavior of $W^{u,H}_{L_2}$ in the region $y < -\bar{k}$. First of all we study (4.2) suppressing the terms containing the factor $(x^2 + y^2)^{-3/2}$. We get the linear equations

$$\ddot{x} - 2\dot{y} = 3x, \qquad \ddot{y} + 2\dot{x} = 0. \tag{4.3}$$

The solution is given by

$$\begin{aligned} x &= \tfrac{2}{3}N + M\cos(t - t_o), \\ y &= B - Nt - 2M\sin(t - t_o). \end{aligned} \tag{4.4}$$

We note that the constants M and N can be computed through

$$M^2 = \dot{x}^2 + \ddot{x}^2, \qquad N = 3(2x + \dot{y}), \tag{4.5}$$

and B, t_o through

$$B = y + (6x + 3\dot{y})\,t - 2\dot{x}, \qquad t - t_o = \arctan(-\ddot{y}/2\ddot{x}).$$

We return to the full equations (4.2) in order to estimate the effect of the previously neglected terms. We take M and N as function of t and we obtain

$$\dot{N} = -3yr^{-3}, \qquad (M^2)^{\cdot} = 2\ddot{x}[-2yr^{-3} - \dot{x}r^{-3} + 3x(x\dot{x} + y\dot{y})\,r^{-5}],$$

where $r^2 = x^2 + y^2$. The limit conditions for M, N follow from the values at L_2 and are $M(-\infty) = 0$, $N(-\infty) = 6 \cdot 3^{-1/3}$.

For the other constants the variation is given by

$$\begin{aligned} \dot{B} &= (2x - 3yt)\,r^{-3}, \\ \dot{t}_o &= 1 - 2(\ddot{y}\dddot{x} - \ddot{y}\dddot{x})(4\ddot{x}^2 + \ddot{y}^2)^{-1} \\ &= [r^{-3}(6\dot{x}y - 6x\dot{y} + 4\dot{x}^2 - 4\dot{y}^2) + r^{-5}(x\dot{x} + y\dot{y})(18xy + 12y\dot{y} - 12x\dot{x}) \\ &\quad + r^{-6}(3y^2 + 2y\dot{x} + 2x\dot{y}) + r^{-8}(-12xy)(x\dot{x} + y\dot{y})] \\ &\quad \cdot [4M^2 + r^{-3}4\dot{x}y + r^{-6}y^2]^{-1}. \end{aligned}$$

Therefore the contribution of the terms containing the factor $(x^2 + y^2)^{-3/2}$ to the coefficients M, N, t_o and B when y goes from $-\bar{k}$ to $-L$ $(L > \bar{k})$ is $O(\bar{k}^{-2})$, $O(\bar{k}^{-1})$, $O(\bar{k}^{-2})$ and $O(\ln(L/\bar{k}))$, respectively, for $\bar{k}$ large.

We note that the three first coefficients go asymptotically to some finite value when $t \to \infty$. This is also true for the averaged value of $\dot{y}$ which equals

$$\lim_{t \to \infty} \dot{B}(t) - N(t) - \dot{N}(t)\, t = \lim_{t \to \infty} -N(t) = -N(\infty).$$

Therefore, the asymptotic behavior of the "waves" of $W^{u,H}_{L_2}$ is given by

$$(\tfrac{2}{3}N(\infty) + M(\infty)\cos t,\ -N(\infty)\, t - 2M(\infty)\sin t).$$

The length of one wave between two consecutive minima of x is given by $\Delta y = 2\pi N(\infty)$, the width $x_{\max} - x_{\min}$ by $2M(\infty)$ (see Fig. 4.4) and the distance to the z.v.c. by $\frac{2}{3}N(\infty) - M(\infty) - 3^{1/6}$.

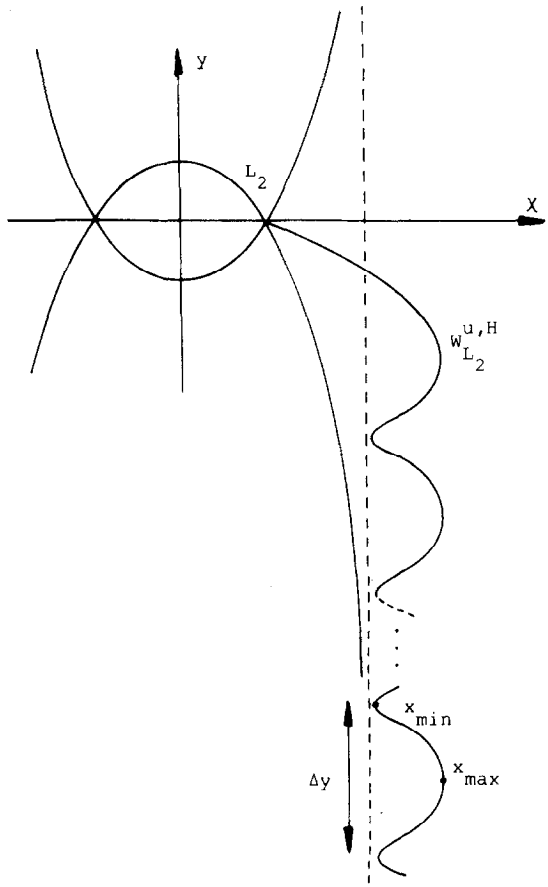

FIG. 4.4. Projection of the right branch of the unstable manifold of L_2 for the Hill's problem near L_2 and far away.

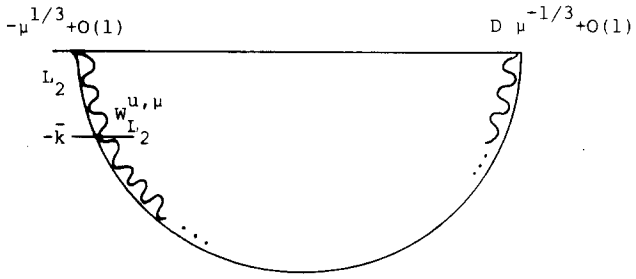

FIG. 4.5. Projection of the right branch of the unstable manifold of L_2 for the RTBP.

Now we study what happens with $W^{u,\mu}_{L_2}$. The main idea is as follows: Given a sufficiently small μ, we take a large value of $\bar{k}$ (it can depend on μ). We get an approximate expression for $W^{u,H}_{L_2}$ up to $y=-\bar{k}$ and from (4.1) an approximation of $W^{u,H}_{L_2}$ from L_2 to $y=-\bar{k}$. The remaining part of this branch of $W^{u,\mu}_{L_2}$ until it again reaches $y=0$ is approximated by the S2BP. The z.v.c. for the RTBP through L_2 when expressed in the scaled variables is nearly a circle (except in a neighborhood of L_2) of radius $\mu^{-1/3}-3^{1/6}+O(\mu^{1/3})$ (see Fig. 4.5).

We recall that both the dominant terms (4.3) of Hill's differential equations for r large and the two-body problem in suitable coordinates (Levi–Civita transformation) are linear with eigenvalues of the Jacobian with zero real part. Therefore, the effect of slight perturbations of the vector field bounded by α acting along a time bounded by β produces changes in the solution essentially bounded by $\alpha\cdot\beta$ (use the variational equations and bound the effect during a finite time).

Let $\bar{\bar{k}}$ be a large fixed value. For $W^{u,H}_{L_2}$ we take the origin of time when $y=-\bar{\bar{k}}$ and for this moment constants $M(0)$, $N(0)$, $t_o(0)$ and $B(0)$ are defined. Let $\bar{k}=\mu^{-1/12}\gg\bar{\bar{k}}$. The time needed to reach $y=-\bar{k}$ is $O(\mu^{-1/12})$. By the analyticity of $W^{u,\mu}_{L_2}$ with respect to $\mu^{1/3}$, for $t=0$ the distance between $W^{u,\mu}_{L_2}$ and $W^{u,H}_{L_2}$ is $O(\mu^{1/3})$. From $t=0$ until $t=O(\mu^{-1/12})$ the terms in (4.1) not present in (4.2) are bounded by $O(\mu^{1/3}\cdot\mu^{-2/12})=O(\mu^{1/6})$. Therefore this originates an error in the estimates about $W^{u,\mu}_{L_2}$ when we replace it by $W^{u,H}_{L_2}$ of the order of $\mu^{1/12}$ up to $y=-\bar{k}$.

Going backwards through the scaling we have

$$\Delta y=2\pi N(\infty)\,\mu^{1/3}(1+O(\mu^{1/12}))$$

as the length of the wave near $y=-\bar{k}\mu^{1/3}=\mu^{1/4}$. From this point on, the motion can be thought of as a S2BP plus perturbations. The limiting S2BP motion is obtained from the limit waves for the Hill problem and corresponds to a semiaxis

$$a=1-(\tfrac{2}{3}N(\infty)-3^{-1/3})\,\mu^{1/3}(1+o(1))$$

and eccentricity $e = M(\infty)\,\mu^{1/3}(1+o(1))$. The time needed to reach the point D (see Fig. 4.5.) is $O(\mu^{-1/3})$. From (1.1) it is seen that the difference between the RTBP and the S2BP that we get when we put $\mu = 0$ in the equations is essentially $\mu \cdot O((x+1-\mu)\,r_2^{-3},\ y r_2^{-3})$. We have $x^2+y^2 = 1+O(\mu^{1/3})$ because the z.v.c. is at a distance from the origin $1-\mu^{1/3}3^{1/6}(1+o(1))$ and $|y| > \mu^{1/4}$ for negative x. Then the difference is bounded by $O(\mu^{1/2})$ and hence the error between approximated positions and the exact ones is $O(\mu^{1/6})$. We must add the effect of the transport of the error between $W^{u,\mu}_{L_2}$ and $W^{u,H}_{L_2}$ from the line $y = -\bar{k}$ to the point D. Again, due to the fact that the variational equations for the S2BP have all the eigenvalues with zero real part, the error obtained is $O(\mu^{1/12})$. Then, the total error is $O(\mu^{1/12})$.

Another error in the computation of the number of waves of $W^{u,\mu}_{L_2}$ until D is introduced by the value of B at $y = -\bar{k}$, which is $O(\ln \mu)$. So, the expression of the semiwaves number, *swn*, is as follows:

$$\begin{aligned} swn &= 2\pi(1+O(\mu^{1/3})+O(\mu^{1/12})+O(\mu^{1/3}\ln\mu))/(2\pi N(\infty)\,\mu^{1/3}(1+O(\mu^{1/12}))) \\ &= N(\infty)^{-1}\mu^{-1/3}(1+O(\mu^{1/12})). \end{aligned} \tag{4.6}$$

When the number of semiwaves is an integer n, by symmetry we get a homoclinic orbit. It follows immediately that this happens for values $\mu_n = n^{-3}N(\infty)^{-3}(1+O(n^{-1/4}))$. This ends the proof of Theorem A.

To get more quantitative information we need the values of $N(\infty)$, $M(\infty)$. A numerical computation starting on $W^{u,H}_{L_2}$ locally near L_2, integration of (4.2) and formulae (4.5) give the values $N(\infty) = 5.1604325\cdots$, $M(\infty) = 2.1330587\cdots$. We realize that the check $N(\infty)^2/3 - M(\infty)^2 = C^H(L_2) = 3^{4/3}$ is satisfied.

Now we study the invariant manifolds of the Lyapunov periodic orbit near L_2. Our objective is to obtain the first intersection of $W^u_{\text{p.o.}}$ on the manifold of Jacobi constant equal to C (C slightly less than $C_2(\mu)$) with the plane $y = 0$ in the region $x > 0$. Suppose that this intersection is a closed curve γ in the variables $x, \dot{x}$. Let S_x be the symmetry with respect to the x axis on this plane. Then, due to the reversibility of the RTBP, $W^s_{\text{p.o.}} \bigcap_{1^{\text{st}}} \{y = 0, x > 0\} = S_x\gamma$. Points P in γ with $\dot{x} = 0$ correspond to (symmetric) orbits homoclinic to the p.o. If γ is transversal to $S_x\gamma$ at P then the homoclinic orbit is transversal. If $\gamma \cap S_x\gamma - \{\dot{x} = 0\} \neq \varnothing$, then nonsymmetric homoclinic orbits appear. However, we shall confine mainly to the symmetric case.

For Hill's problem and $C^H \lesssim 3^{4/3}$ a Lyapunov periodic orbit is known to exist. Linearizing (4.2) near L_2^H we get

$$\ddot{z} - 2\dot{y} = 9z,$$

$$\ddot{y} + 2\dot{z} = -3y,$$

where $z = x - x_{L_2^H}$. The expression of the linear part of the p.o. is given by

$$z = a \cos st,$$

$$y = b \sin st,$$

with $s = (2 \cdot 7^{1/2} - 1)^{1/2}$, $b = -(9 + s^2)\, a/(2s)$, $a = (\Delta C^H (18 + 4s^2)^{-1})^{1/2}$, where $\Delta C^H = 3^{4/3} - C^H$. Therefore the p.o. projects on the (x, y) plane near an ellipse around L_2^H of size proportional to $(\Delta C^H)^{1/2}$. This p.o. is hyperbolic and we consider the unstable manifold $W^{u,H}_{\text{p.o.}}$ associated to it. The intersection of $W^{u,H}_{\text{p.o.}}$ with $y = 0$ is again near an ellipse in the plane $x, \dot{x}$ of area $(\pi/s) \cdot \Delta C^H$.

Using the same argument that was employed for $W^{u,H}_{L_2}$, one of the branches of $W^{u,H}_{\text{p.o.}}$ goes down to the right and near the z.v.c. (Fig. 4.6), crossing the line $y = -\bar{k}$ for any fixed value of $\bar{k}$. Using the linear flow near the equilibrium point (see Section 2), the fact that ΔC^H is small and variational equations along $W^{u,H}_{L_2}$ for a finite time, the intersection of $W^{u,H}_{\text{p.o.}}$ with $y = -\bar{k}$ is roughly an ellipse E with center at $W^{u,H}_{L_2} \cap \{y = -\bar{k}\}$. We remark that the same is true for the RTBP because it is an arbitrarily small perturbation of Hill's one if μ is small enough (recall Eq. (4.1)).

In the scaled variables the Jacobi constant $\bar{C} = C^H + O(\mu^{1/3})$ equals

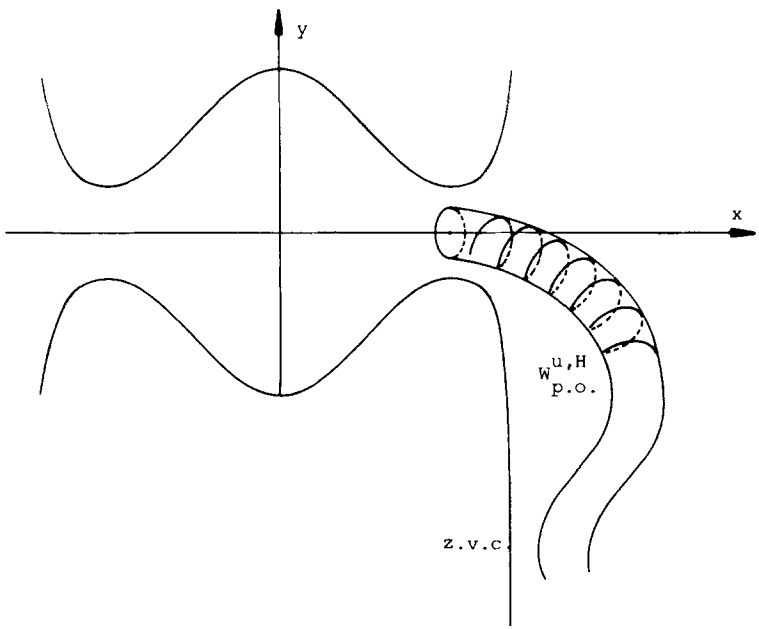

FIG. 4.6. Qualitative picture of the right branch of the unstable manifold of the Lyapunov p.o. associated to L_2.

$(C-3)\mu^{-2/3}$. Then $\Delta C = \mu^{2/3}\,\Delta\bar{C} \simeq \mu^{2/3}\,\Delta C^H$ and the semiaxes of the p.o. and the ellipse E in the usual synodic coordinates are $O(\mu^{1/3}(\Delta C^H)^{1/2})$.

Now we wish to study the different cuts of $W^{u,H}_{\text{p.o.}}$ with planes $y=-\bar{k}$ when $\bar{\bar{k}}>\bar{k}$ changes. If the value of $\bar{k}$ is large, Hill's equations (4.2) are well approximated by the linear equations (4.3). We know that $W^{u,H}_{L_2}$ is asymptotically expressed by (4.4) when $M=M(\infty)$, $N=N(\infty)$ and B, t_o are suitable values.

For the sake of simplicity we take a value of $\bar{k}$ such that $W^{u,H}_{L_2}$ has a maximum of x when this manifold intersects $y=-\bar{k}$. This means that for this orbit $t_0=0$ in (4.4) if we put $t=0$ at the moment of crossing $y=-\bar{k}$.

Let ξ, $\dot{\xi}$ be the rectangular coordinates on the plane $y=-k$, $\bar{k}\leqslant k\leqslant\bar{\bar{k}}$, defined by $\xi = x - x^H_{L_2}(k)$, $\dot{\xi} = \dot{x} - \dot{x}^H_{L_2}(k)$, where $x^H_{L_2}(k)$ (resp. $\dot{x}^H_{L_2}(k)$) is the coordinate x (resp. $\dot{x}$) of $W^{u,H}_{L_2}\cap\{y=-k\}$.

As we said before $E = W^{u,H}_{\text{p.o.}}\cap\{y=-\bar{k}\}$ has dominant terms which can be parameterized as

$$\begin{aligned}\xi &= \rho(\cos\gamma\cos\sigma - A\sin\gamma\sin\sigma),\\ \dot{\xi} &= \rho(\sin\gamma\cos\sigma + A\cos\gamma\sin\sigma),\end{aligned}\tag{4.7}$$

where A, γ, ρ are constants (depending on $\bar{k}$, μ, ΔC^H) and σ is a parameter.

We look for the linear map T_{t^*} which sends $(\xi,\dot{\xi})$ on the plane $y=-\bar{k}$ to $(\xi^*,\dot{\xi}^*)$ on the plane $y=-\bar{\bar{k}}$. The value t^* means the time required for $W^{u,H}_{L_2}$ by going from $y=-\bar{k}$ to $y=-\bar{\bar{k}}$.

Let M, N, B, t_o be the values of the constants in (4.4) for some point in E. For $\bar{k}$ large the Jacobi constant for the Hill problem is $C^H \simeq 3x^2 - \dot{x}^2 - \dot{y}^2 = N^2/3 - M^2$. Therefore if $M = M(\infty) + \Delta M$, $N = (\infty) + \Delta N$, we have $\Delta C^H \simeq \frac{2}{3}N(\infty)\,\Delta N - 2M(\infty)\,\Delta M$.

Let $P_1\in E$ such that $\dot{\xi}=0$, $\xi>0$ and $P_2\in E$ such that $\xi=0$, $\dot{\xi}>0$. In order to obtain T_{t^*} it is enough to find the images $T_{t^*}P_1$ and $T_{t^*}P_2$.

For P_1, for instance, we find σ and then ξ as a function of γ, A, ρ. Therefore the constants M, N, B, t_o are available. We look for a final time $t=t^*+\Delta t$ such that the orbit starting at P_1 when $t=0$ reaches $y=-\bar{\bar{k}}$. For this final time we compute $(\xi^*,\dot{\xi}^*)$. Then we note that terms in ρ and in ΔC^H appear and the first ones are dominant since $\Delta C^H = O(\rho^2)$. In the same way we proceed with P_2. This gives us the matrix

$$T_{t^*} = \frac{1}{(N+2M\cos t^*)(N+2M)}\tag{4.8}$$

$$\times\begin{pmatrix} 4MN + (4M^2+N^2)\cos t^* + 3M^2 t^*\sin t^* & (2M+N)^2\sin t^* \\ -N^2\sin t^* + 3M^2 t^*\cos t^* & 2(M+N)^2\cos t^*\end{pmatrix},$$

where from now on M, N stand for $M(\infty)$, $N(\infty)$. This map is area preser-

ving and the nonperiodic terms in t^* produce an averaged linear increase of the maximum eigenvalue with respect to t^*.

As a conclusion the ellipse E, i.e., the sections $W^{u,H}_{\text{p.o.}} \cap \{y = -k\}$ when k increases, rotate and one of the axes increases (on the average) but the area of E is preserved.

For $t^* = 2n\pi$ (maxima of x on $W^{u,H}_{L_2}$) and $t^* = (2n+1)\pi$ (minima of x on $W^{u,H}_{L_2}$), we get

$$T_{2n\pi} = \begin{pmatrix} 1 & 0 \\ \left(\dfrac{3M}{N+2M}\right)^2 2n\pi & 1 \end{pmatrix},$$

$$T_{(2n+1)\pi} = \begin{pmatrix} \dfrac{2M-N}{2M+N} & 0 \\ -\dfrac{3M^2}{N^2-4M^2}(2n+1)\pi & \dfrac{2M+N}{2M-N} \end{pmatrix}.$$

If we recall that we are dealing with the RTBP the situation is the following one: for some large values of $k > 0$ and μ small, $-k\mu^{1/3}$ is small. On $y = -k\mu^{1/3}$ the section of $W^{u,\mu}_{\text{p.o.}}$ is roughly an ellipse with center at the intersection of $W^{u,\mu}_{L_2}$ with the plane $y = -k\mu^{1/3}$ (we consider each one of the manifolds on its corresponding level of Jacobi constant). This ellipse has area proportional to ΔC and the major axis rotates and increases (on the average) when k does.

In order to study the first cut γ of $W^{u,\mu}_{\text{p.o.}}$ with $y = 0$, $x > 0$ we can approximate the RTBP by the S2BP if k is large enough as we did with $W^{u,\mu}_{L_2}$. As a matter of fact, instead of taking an ellipse on $y = -k\mu^{1/3}$, $x < 0$ and studying the image under S2BP on $y = 0$, $x > 0$, we can suppose that initially we have the ellipse on $y = 0$, $x < 0$. Taking into account the rotation of the ellipse it is not restrictive to suppose that the axes of it are parallel to the x and $\dot{x}$ axes in order to simplify the computations. Therefore we start with the initial conditions

$$\begin{aligned} x &= -1 + \mu + (\tfrac{2}{3}N + M\cos\tau)\,\mu^{1/3} + k_1\,\Delta C^{1/2}\cos\sigma, \\ \dot{x} &= (-M\sin\tau)\,\mu^{1/3} + k_2\,\Delta C^{1/2}\sin\sigma, \\ y &= 0, \end{aligned} \tag{4.9}$$

and $\dot{y}$ is obtained from the Jacobi relation as

$$\begin{aligned} \dot{y} = {} & (-N - 2M\cos\tau)\,\mu^{1/3} \\ & - (N + 2M\cos\tau)^{-1}[(2N + 3M\cos\tau)\,k_1\,\Delta C^{1/2}\cos\sigma \\ & + M(\sin\tau)\,k_2\,\Delta C^{1/2}\sin\sigma]. \end{aligned}$$

Here k_1, k_2 are finite quantities related to the axes and σ is the parameter of a point in the ellipse. The parameter τ is related to the time for which $W^{u,H}_{L_2}$ reaches again $y=0$, $x<0$ when we start at $y=-k\mu^{1/3}$ and go back skipping the nonlinear terms in (4.2). (In fact y is not exactly zero because we select τ with the smallest $|y|$ such that the ellipse is in suitable position as given by the first two equations of (4.9).)

We recall that μ_k is a value of μ for which $W^{u,\mu}_{L_2} \equiv W^{s,\mu}_{L_2}$ (right branches). Let us introduce the factors $\bar{\alpha}$, $\bar{\beta}$ given by

$$\begin{aligned} \mu &= \mu_k + \bar{\alpha}\mu_k^{4/3}, \\ \Delta C &= \bar{\beta}\mu_k^{4/3}, \end{aligned}$$

where $\bar{\alpha}$, $\bar{\beta} = O(1)$ will be taken as variables in the sequel instead of μ, ΔC.

Then, up to terms in $\mu_k^{2/3}$ we have in (4.9)

$$\begin{aligned} x_0 &= -1 + (\tfrac{2}{3}N + M\cos\tau)(\mu_k^{1/3} + \tfrac{1}{3}\mu_k^{2/3}\bar{\alpha}) + k_1\mu_k^{2/3}\bar{\beta}^{1/2}\cos\sigma, \\ \dot{x}_0 &= (-M\sin\tau)(\mu_k^{1/3} + \tfrac{1}{3}\mu_k^{2/3}\bar{\alpha}) + k_2\mu_k^{2/3}\bar{\beta}^{1/2}\sin\sigma, \\ y_0 &= 0, \\ \dot{y}_0 &= (-N - 2M\cos\tau)(\mu_k^{1/3} + \tfrac{1}{3}\mu_k^{2/3}\bar{\alpha}) \\ &\quad - (N + 2M\cos\tau)^{-1}[(2N + 3M\cos\tau)\, k_1\mu_k^{2/3}\bar{\beta}^{1/2}\cos\sigma \\ &\quad + M(\sin\tau)\, k_2\mu_k^{2/3}\bar{\beta}^{1/2}\sin\sigma], \end{aligned} \tag{4.10}$$

where the subindex 0 means that we take the time equal to zero, $t=0$, at this moment.

Note that if $\bar{\alpha}=\bar{\beta}=0$ on (4.10) we are on a homoclinic orbit to L_2 which cuts $y=0$, $x>0$ with $\dot{x}=0$. We try to see the variations in x, $\dot{x}$ that we obtain when $\bar{\alpha}$, $\bar{\beta}$ and σ change.

Let $\mathbf{r}_0$, $\dot{\mathbf{r}}_0$, be the initial conditions for the two-body problem (2BP) in sidereal coordinates and $r_0 = |\mathbf{r}_0|$, $v_0 = |\dot{\mathbf{r}}_0|$, $r_0\dot{r}_0 = (\mathbf{r}_0, \dot{\mathbf{r}}_0)$. We have $\dot{\mathbf{r}}_0 = \begin{pmatrix} \dot{x}_0 - y_0 \\ \dot{y}_0 + x_0 \end{pmatrix}$. Then the Keplerian elements of the orbit can be determined by the formulas

$$\begin{aligned} \frac{1}{a} &= \frac{2}{r_0} - v_0^2, \\ e\cos E_0 &= r_0 v_0^2 - 1, \\ e\sin E_0 &= r_0\dot{r}_0 a^{-1/2}, \\ V_0 + \omega &= \operatorname{Arg}\mathbf{r}_0, \end{aligned} \tag{4.11}$$

where a, e, ω denote the semimajor axis, the eccentricity and the argument

of pericenter, respectively. E_0, V_0 and M_0 are the eccentric, true and mean anomalies, related by

$$\begin{aligned} E &= M + e \sin M + e^2 \sin M \cos M + O(e^3), \\ V &= E + e \sin E + \frac{e^2}{2} \sin E \cos E + O(e^3). \end{aligned} \tag{4.12}$$

We note that formulae (4.11) are accurate up to terms $O(\mu^{2/3})$ because we take the mass of the primary equal to 1 instead of 1-μ. For our purpose it is enough to perform almost all the computations with an error $O(\mu)$.

After some time t_f an orbit with initial conditions (4.10) reaches $y=0$, $x>0$, in synodic coordinates, for the first time. From

$$M_f = M_0 + nt_f, \tag{4.13}$$

where n is the mean motion ($n^2a^3=1$), and (4.12) we determine t_f through the relation

$$V_f + \omega = t_f. \tag{4.14}$$

When t_f is obtained we get x, $\dot{x}$ from

$$\begin{aligned} x_f &= a(1 - e \cos E_f) \\ \dot{x}_f &= \sqrt{a}\, e \sin E_f \cdot x_f^{-1}. \end{aligned} \tag{4.15}$$

For $W_{L_2}^{\mu,\mu_k}$ we reach $y=0$, $x>0$ at pericenter or apocenter ($\dot{x}=0$). Therefore M_f for this orbit equals 0 or π. Let us suppose it equals the value 0 (similar computations can be done in the case of value π). Let n_w, x_w, t_w denote the values of mean motion, x_f and t_f, respectively, for $W_{L_2}^{\mu,\mu_k}$. A somewhat lengthy, but elementary, computation from (4.10)–(4.15) gives

$$\begin{aligned} x_f - x_w = {} & \mu_k^{1/3} M(1 - \cos M_f) + \mu_k^{2/3} \\ & \times \left\{ -\frac{2MN}{3}(1 - \cos M_f) + M^2 \sin^2 M_f - \frac{2}{9} N\bar{\alpha} \right. \\ & - \frac{M}{3}\bar{\alpha} \cos M_f - \bar{\beta}^{-1/2}(N + 2M \cos \tau)^{-1}(2M + N \cos M_f) \\ & \left. \times (k_1 \cos \tau \cos \sigma - k_2 \sin \tau \sin \sigma) \right\} + O(\mu_k), \end{aligned} \tag{4.16}$$

$$\begin{aligned} \dot{x}_f = {} & \sin M_f \left[\mu^{1/3} M + \mu^{2/3} \right. \\ & \times \left\{ \frac{MN}{3} + 2M^2 \cos M_f + \frac{M}{3}\bar{\alpha} + \bar{\beta}^{1/2} N (N + 2M \cos \tau)^{-1} \right. \\ & \left. \left. \times (k_1 \cos \tau \cos \sigma - k_2 \sin \tau \sin \sigma) \right\} \right] + O(\mu_k), \end{aligned}$$

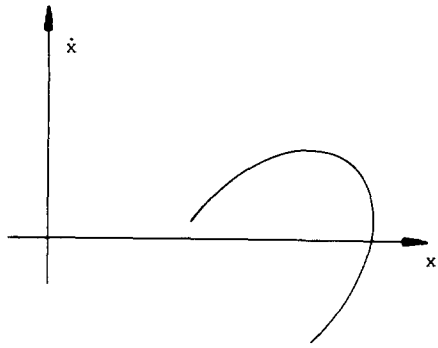

FIG. 4.7. Section of $W^{u,S}_{\text{p.o.}}$ with $y=0$, in $x>0$, up to terms $O(\mu_k^{1/3})$.

where M_f is obtained as the solution of a kind of Kepler equation:

$$\mu_k^{1/3}\left\{\left(\frac{1}{3}N\bar{\alpha}+\bar{\beta}^{1/2}3M(N+2M\cos\tau)^{-1}(k_1\cos\tau\cos\sigma-k_2\sin\tau\sin\sigma)\right)\frac{\pi}{N}\right.$$

$$\left.+NM_f+2M\sin M_f\right\}+O(\mu_k^{2/3}, t_w\mu_k, n_w-1-N\mu_k^{1/3})=0. \tag{4.17}$$

Theorem B will follow from a careful examination of (4.16), (4.17). Given $\bar{\alpha}, \bar{\beta}$ when σ ranges from 0 to 2π, from (4.17) we get different values of M_f. The range of variation of M_f depends on $\bar{\alpha}, \bar{\beta}$. By substitution of these values on (4.16) we obtain, including only terms in $\mu_k^{1/3}$, an arc of circumference of diameter $2M\mu_k^{1/3}$ travelled twice (Fig. 4.7).

This arc has one end on $\dot{x}=0$ (this implies homoclinic tangency up to terms of higher order) if and only if for some $M_f=j\pi$ we have

$$\left.\frac{dM_f}{d\sigma}\right|_{M_f=j\pi}=0$$

in (4.17). This is accomplished if and only if

$$\bar{\beta}=L(\bar{\alpha}+3jN)^2, \tag{4.18}$$

with $L=N^2(N+2M\cos\tau)^2/(81M^2(k_1^2\cos^2\tau+k_2^2\sin^2\tau))$.

The true relation will be $\bar{\beta}=L(\bar{\alpha}+3jN)^2+O(\mu_k^{1/3})$. From the definition of $\bar{\alpha}$ it follows that when $\mu=\mu_{k+j}$ one has $\bar{\alpha}=-3jN+O(\mu_k^{1/3})$. Therefore the set of homoclinic tangencies is obtained for the mesh displayed in Fig. 4.8.

The numbers in Fig. 4.8 show the number of symmetric homoclinic points found in the first intersection of $W^{u,\mu}_{\text{p.o.}}$ with $y=0$, $x>0$ when changing μ and ΔC. The total number of homoclinic points is the double.

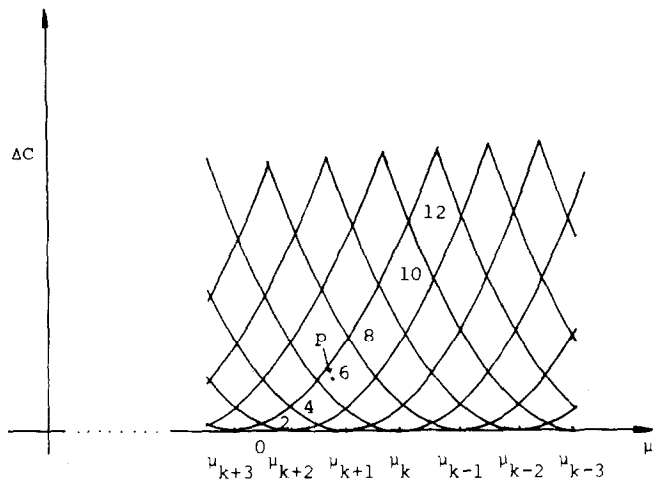

FIG. 4.8. Partition of the $(\mu, \Delta C)$ plane according to the number of transversal symmetric (1, 1)-h.o. to the Lyapunov p.o. associated to L_2.

To discuss the effect of the terms in $\mu_k^{2/3}$ we put $\dot{x}_f = 0$ in (4.16). Then $M_f = j\pi$ and

$$x_f - x_w = \mu_k^{1/3} M(1-(-1)^j) + \mu_k^{2/3} \left\{ -\frac{2MN}{3}(1-(-1)^j) - \frac{2}{9}N\bar{\alpha} - \frac{M}{3}\bar{\alpha}(-1)^j \right.$$
$$\left. - \bar{\beta}^{1/2} \frac{2M+(-1)^j N}{N+2M\cos\tau}(k_1 \cos\tau\cos\sigma - k_2 \sin\tau\sin\sigma) \right\} + O(\mu_k), \tag{4.19}$$

$$\frac{1}{3}\pi\bar{\alpha} + \bar{\beta}^{1/2} \frac{3M\pi}{N(N+2M\cos\tau)}(k_1\cos\tau\cos\sigma - k_2\sin\tau\sin\sigma) + Nj\pi$$
$$= O(\mu_k^{1/3}). \tag{4.20}$$

Provided $\bar{\beta}$ is large enough (4.20) can be solved for σ as a function of j. The number of solutions is given in Fig. 4.8. Solving (4.20) and inserting the obtained value of σ in (4.19) gives

$$x_f - x_w = \mu_k^{1/3} M(1-(-1)^j + \mu_k^{2/3} \left\{ -\frac{2MN}{3}(1-(-1)^j) - \frac{2}{9}N\bar{\alpha} - \frac{M}{3}\bar{\alpha}(-1)^j \right.$$
$$\left. + \frac{2M+(-1)^j N}{3M}(Nj + \bar{\alpha}/3)\,N \right\} + O(\mu_k). \tag{4.21}$$

If j is even then

$$x_f - x_w = \mu_k^{2/3} \left\{ -\frac{2}{9} N\bar{\alpha} - \frac{M}{3}\bar{\alpha} + \frac{2M+N}{3M}(Nj + \bar{\alpha}/3)\, N \right\} + O(\mu_k).$$

A change of two units in j produces a change $\Delta_e = \mu_k^{2/3}((2M+N)/3M)\, 2N^2$ in $x_f - x_w$.

If j is odd then

$$x_f - x_w = 2M\mu_k^{1/3} + \mu_k^{2/3} \times \left\{ -\frac{4MN}{3} - \frac{2}{9} N\bar{\alpha} + \frac{M}{3}\bar{\alpha} + \frac{2M-N}{3M}(Nj + \bar{\alpha}/3)\, N \right\} + O(\mu_k).$$

A change of two units in j produces a change $\Delta_o = \mu_k^{2/3}((2M-N)/3M)\, 2N^2$ in $x_f - x_w$.

Therefore, including terms $O(\mu_k^{2/3})$ the curve obtained by intersection of $W^{u,\mu}_{\text{p.o.}}$ with $y=0$, $x>0$ is a kind of spiral, as shown in Fig. 4.9, travelled twice.

The length depends on the size of $\bar{\beta}$. For large $\bar{\beta}$ the range of M_f is roughly $\pi 6MN^{-2}(N+2M\cos\tau)^{-1}(k_1^2\cos^2\tau + k_2^2\sin^2\tau)^{1/2}\beta^{1/2}$. Note that according to the values of M, N, $\Delta_e \simeq 78.457\ \mu_k^{2/3}$, $\Delta_o \simeq -7.444\ \mu_k^{2/3}$.

We had to show that the curve in Fig. 4.9 is not orhtogonal to the x axis on the points $\dot{x}=0$. From (4.16), (4.17) it follows that

$$\left.\frac{dx}{d\dot{x}}\right|_{M_f = j\pi} = \mu_k^{1/3} \frac{N}{3M^2\pi}(2M + (-1)^j N)^2 + O(\mu_k^{2/3}).$$

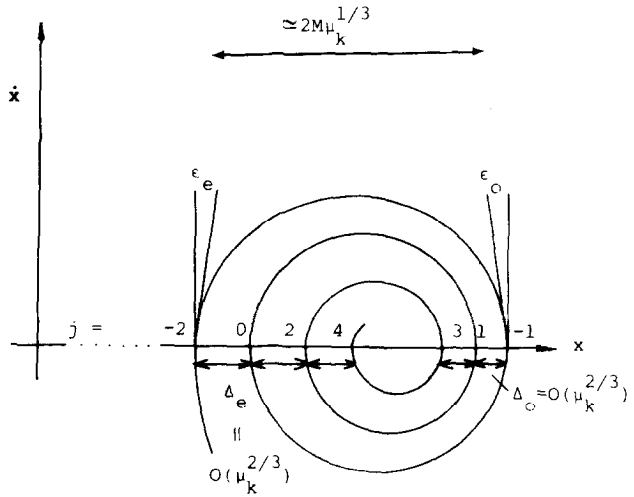

FIG. 4.9. Section of $W^{u,S}_{\text{p.o.}}$ with $y=0$, in $x>0$, up to terms $O(\mu_k^{2/3})$.

For j even we find

$$\varepsilon_e = \left.\frac{dx}{d\dot{x}}\right|_{M_f = j\pi} \simeq 10.693\ \mu_k^{1/3}$$

and for j odd

$$\varepsilon_0 = \left.\frac{dx}{d\dot{x}}\right|_{M_f = j\pi} \simeq 0.096\ \mu_k^{1/3}.$$

To end the description of the section of $W^{u,\mu}_{\text{p.o.}}$ we only need to say that the area enclosed by the section is $O(\mu_k^{4/3})$. (In fact, it is roughly $(\pi/s)\,\Delta C$.) Therefore the "width" of the spiral is $O(\mu_k)$ (see Fig. 4.10). Figure 4.10 corresponds to a point P as shown in Fig. 4.8.

Point Q in Fig. 4.10 shows roughly the intersection $(x_f, \dot{x}_f)$ of $W^{u,\mu}_{L_2}$ for the same value of μ (i.e., putting $\bar{\beta} = 0$ and keeping $\bar{\alpha}$ fixed). It is not necessarily true that Q belongs to the region bounded by the section of $W^{u,\mu}_{\text{p.o.}}$.

As a conclusion the homoclinic points are transversal except, perhaps, in a neighborhood of width $O(\mu_k^{1/3})$ of the curves (4.18).

The same is true for the nonsymmetric homoclinic points shown in Fig. 4.11, *A*, *B*.

Only a few words are required to look for the effect of the neglected

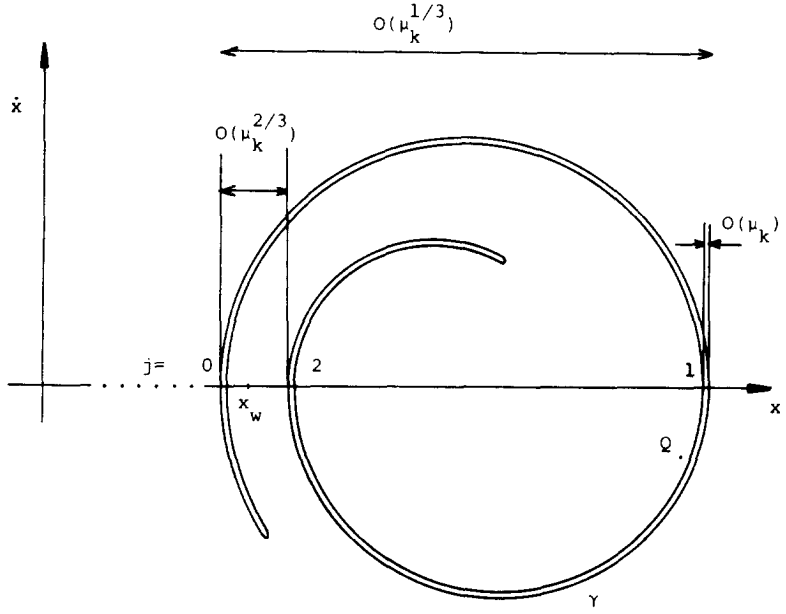

FIG. 4.10. Section of $W^{u,S}_{\text{p.o.}}$ with $y = 0$, in $x > 0$, up to terms $O(\mu_k)$.

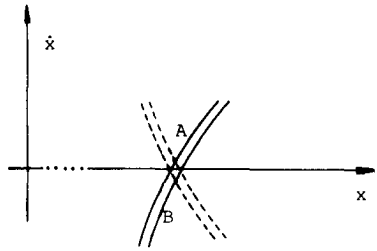

FIG. 4.11. Nonsymmetric (1, 1)-homoclinic points.

terms. They come from the fact that the starting ellipse in (4.9) is not the true curve. This true curve contains cubic terms and therefore of the order μ_k, but all those terms were skipped on (4.11) because we only need terms up to $\mu_k^{2/3}$ for the theorems. This concludes the proof of Theorem B.

5. NUMERICAL RESULTS

In order to check the analytical results obtained and to get more information we have done several numerical computations.

First we look for $W_{L_2}^{u,S}$ (which in this case is an asymptotic orbit) as a function of μ. The stable manifold is obtained by symmetry. We compute the first intersection Q with the plane $y=0$. Let α be the angle between the velocity at that point and the positive y axis (in the clockwise sense), see Fig. 5.1 (obtained for $\mu=\bar{\mu}_k=0.3808139842\cdot 10^{-2}$, see later). When $\alpha=0$ we have $W_{L_2}^{u,S}\equiv W_{L_2}^{s,S}$ and therefore these coincident invariant manifolds become a homoclinic orbit. The first values of μ_k, $k\geqslant 2$, of μ for which $\alpha=0$ are given in Table I. The same table gives some values $\bar{\mu}_k$, $k\geqslant 0$, for which α is an extremum and the corresponding value of $\tan\alpha$. For k odd $\alpha(\bar{\mu}_k)$ is a maximum and for k even it is a minimum (k is the number of semiwaves). Note that according to Section 4 the asymptotical behavior of the values of μ_k, $\bar{\mu}_k$ is

$$\mu_k = k^{-3}N^{-3}(1+o(1)) \simeq 0.007276821\, k^{-3},$$

$$\bar{\mu}_k = \left\{2[k/2]\, N - \frac{N}{\pi}(-1)^k \arccos\left(-\frac{2M}{N}\right) - \frac{2M}{\pi N}(-1)^k (N^2-4M^2)^{1/2}\right\}^{-3}(1+o(1))$$

$$\simeq (5.1604325\, k - 0.2175565)^{-3} \qquad (k \text{ odd})$$

$$\simeq (5.1604325\, k - 4.942876)^{-3} \qquad (k \text{ even}),$$

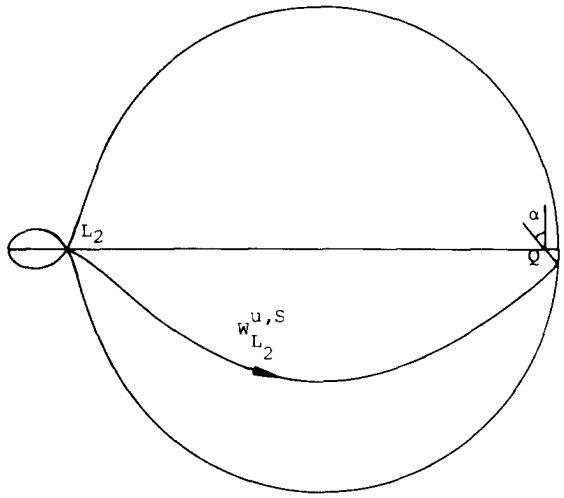

FIG. 5.1. The manifold $W^{u,S}_{L_2}$ for $\mu = \bar{\mu}_2$.

TABLE I

Zeros and Extrema of $\alpha(\mu)$

k	μ_k	$\bar{\mu}_k$	$\tan \alpha(\bar{\mu}_k)$
0		0.98871	0.13632[a]
1		0.4797 *E*-2	1.0176322
2	0.4253863522*E*-2	0.3808139842*E*-2	−0.99130703
3	0.6752539971*E*-3	0.2288475342*E*-3	0.82310415
4	0.2192936884*E*-3	0.2103273193*E*-3	−0.82049541
5	0.971301798 *E*-4	0.525826367 *E*-4	0.78756529
6	0.512551995 *E*-4	0.499753125 *E*-4	−0.78664595
7	0.302775358 *E*-4	0.197092090 *E*-4	0.77245060
8	0.193529253 *E*-4	0.19005625 *E*-4	−0.77198908
9	0.131120186 *E*-4	0.94237676 *E*-5	0.76406657
10	0.92907436 *E*-5	0.91597656 *E*-5	−0.76377536
11	0.68212830 *E*-5	0.52152100 *E*-5	0.75873026
12	0.51549632 *E*-5	0.50953125 *E*-5	−0.75852529
13	0.39900811 *E*-5	0.318175 *E*-5	0.75496354
21	0.8807195 *E*-6	0.7670312 *E*-6	0.745718
22	0.7619792 *E*-6	0.7570312 *E*-6	−0.7460
23	0.6636634 *E*-6	0.584688 *E*-6	0.7476029

[a] For $\mu = 1$ the limit value is $\tan \alpha(1) = 0.13722644$

where M, N stand for $M(\infty)$, $N(\infty)$, [ ] denotes the integer part and arc cos is taken in $(\pi/2, \pi)$. The numerical values are obtained using $M = 2.1330587$, $N = 5.1604325$ as stated in Section 4.

The limiting value of $|\tan \alpha(\bar{\mu}_k)|$ is $M(N^2 - 4M^2)^{-1/2} \simeq 0.7346118$.

Numerical results show good agreement with these figures. An empirical fit for μ_k, $k = 2 \div 13$, gives

$$\mu_k \simeq 0.00728832k^{-3} + 0.01702374k^{-4} + 0.022906k^{-5} + 0.07213k^{-6} + \cdots$$

allowing for predictions for $k = 21, 22, 23$ with relative error less than 5×10^{-4}.

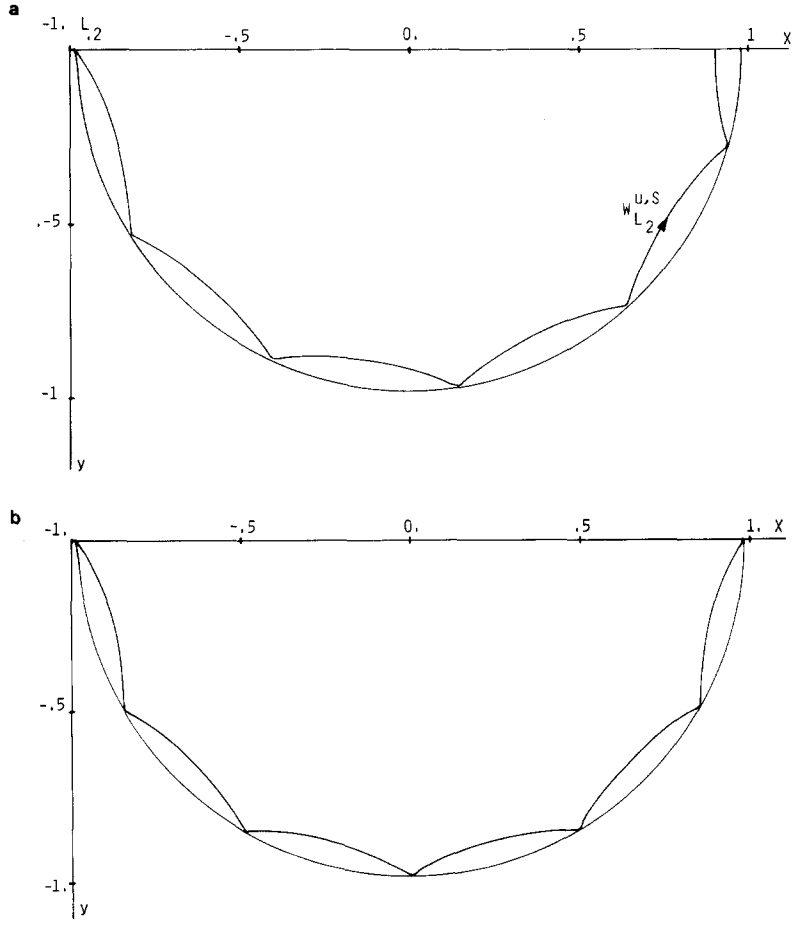

FIG. 5.2. The manifold $W^{u,S}_{L_2}$: (a) for $\mu = \mu_{11}$; (b) for $\mu = \mu_{12}$.

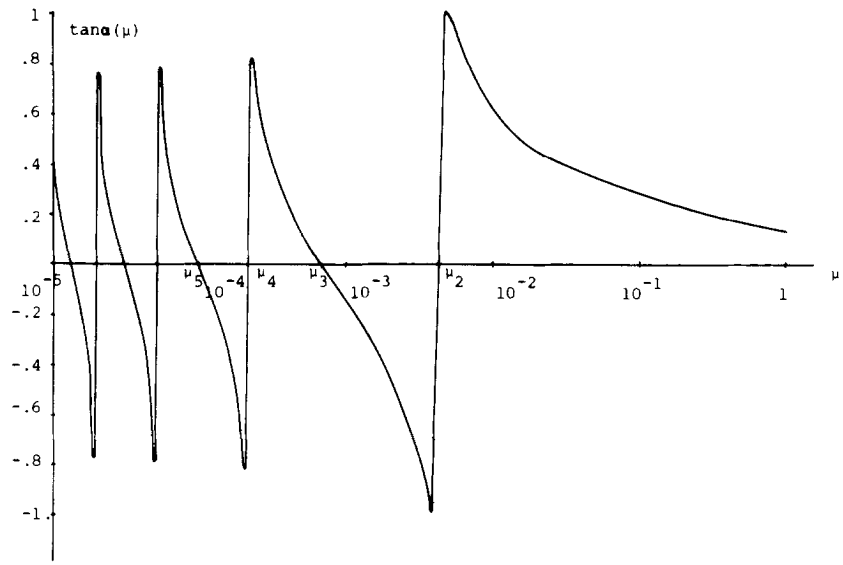

FIG. 5.3. The tangent of the argument of $(\dot{y}, \dot{x})$ when $W^{u,S}_{L_2}$ reaches $y=0$, in $x>0$, as a function of μ.

The h.o. related to L_2 for $\mu=\mu_{10}, \mu_{11}$ are shown in Fig. 5.2. In Fig. 5.1 we used $\mu=\bar{\mu}_2$. A plot of tan α as a function of μ is given in Fig. 5.3. We remark that after $\bar{\mu}_1$ the angle α decreases (with a minor increase near $\mu=1$) without additional zeros. See below, when Hill's case is studied for the limiting value of $\alpha(\mu)$ when $\mu \to 1$. We conclude that for μ small there are no homoclinic orbits in the J region having only one cut with $y=0$.

The next step is the computation of the invariant manifolds of the p.o. of family (c) for several values of μ and several values of C below C_2 but with $\Delta C = C_2 - C$ small. We begin with the computation of the p.o. It can be seen as a hyperbolic fixed point P of the Poincaré map for $y=0$ in the $(x, \dot{x})$ plane. Next the eigenvalues and eigenvectors are obtained. Let V^u and λ be the normalized unstable eigenvector and the related eigenvalue. We look for the curve $\Gamma_1^{u,S}$ intersection of $W^{u,S}_{\text{p.o.}}$ with the $(x, \dot{x})$ plane. This curve (diffeomorphic to S^1 in McGehee's region, see Section 3) can be parameterized by some $z \in [0, 1]$. Let a be some small quantity such that the unstable invariant manifold W^u_p under the Poincaré map is well approximated by its linear part up to a distance a from P. We recall that W^u_p is the intersection of $W^u_{\text{p.o.}}$ with the $(x, \dot{x})$ plane. Therefore the flow transportation of the segment K with extrema $P + aV^u$, $P + a\lambda V^u$ until it reaches the plane $(x, \dot{x})$ in the $\bar{N}_{\text{far}}$ region gives $\Gamma_1^{u,S}$. We merely state that some of the first intersections with the $(x, \dot{x})$ plane must be skipped. The parameter z gives a point in the segment K through $z \to P + a \cdot$

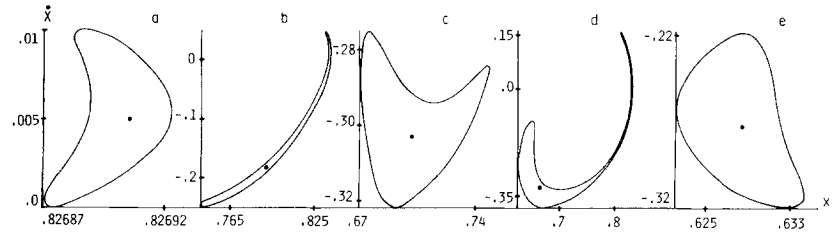

FIG. 5.4. Some first sections of $W^{u,S}_{L_2}$ with $y=0$, $x>0$. Related values of $(\mu, \Delta C)$: (a) (0.004262863522, 0.00000018); (b) (0.0038, 0.00065313); (c) (0.0029, 0.001611341); (d) (0.0027, 0.009686552); (e) (0.0018, 0.000045351).

$\exp(z \cdot \ln \lambda)\, V^u$. In this way equidistributed points z in $[0, 1]$ would produce equidistributed points in $\Gamma^{u,S}_1$ if only linear behavior was present. Figure 5.4 displays some "artistic" cuts $\Gamma^{u,S}_1$ for selected values of (μ, C).

The set of values of μ for which we have an orbit double asymptotic to the critical point L_2 is discrete. Then for any other value of μ the manifold $W^{u,S}_{L_2}$ reaches the $(x, \dot{x})$ plane in a point $(x^*, \dot{x}^*)$ outside the x axis. A plot of $\dot{x}^*$ as a function of μ is given in Fig. 5.5. Therefore, if ΔC is sufficiently small, $\Gamma^{u,S}_1$ does not cut the x axis and hence (by the symmetry) there are no $(1, 1)$-h.p. For a fixed value of μ if we increase ΔC we hope that $\Gamma^{u,S}_1$ becomes larger. Therefore we can look for some value of ΔC such that $\Gamma^{u,S}$ becomes tangent to the x axis for the first time. For that value $\Delta C = \Delta C(\mu)$ we have a tangential (as opposite to transversal) $(1, 1)$-h.o. and in a neighborhood of $\Delta C(\mu)$ (for increasing ΔC) we get $(1, 1)$-transversal homoclinic orbits. The fact that the increase of ΔC produces such transversality has been analytically shown in Section 4 for μ small enough. For the values which we report here this has been checked numerically. It is clear that $\Delta C(\mu_k) = 0$. Table II offers values of $\Delta C(\mu)$ for $\mu \in [0.00023, 0.0042]$.

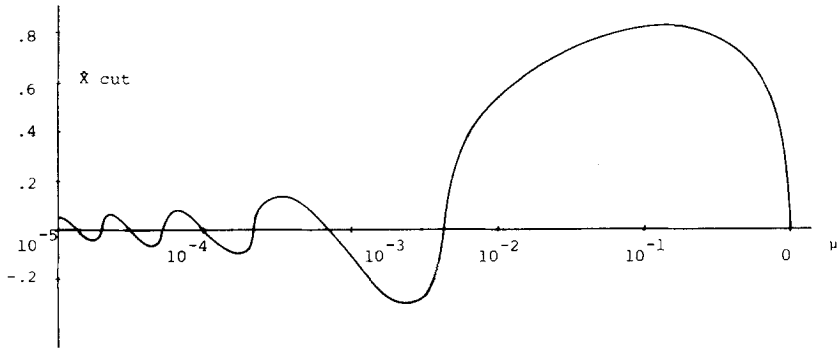

FIG. 5.5. Plot of $\dot{x}$ when $W^{u,S}_{L_2}$ reaches $y=0$, in $x>0$, as a function of μ.

TABLE II

Values of ΔC as a Function of μ for Which Tangential h.o. Exist

μ	ΔC	z	D
0.00023	0.0000103	0.12	0.000514
0.00025	0.0000783	0.13	0.00145
0.0003	0.000454	0.15	0.00366
0.00035	0.00103	0.17	0.00571
0.0004	0.001729	0.20	0.00765
0.00042	0.002035	0.21	0.00833
0.00045	0.00174	0.68	0.00756
0.0005	0.000933	0.66	0.00527
0.00055	0.000428	0.65	0.00340
0.0006	0.000142	0.65	0.00188
0.00065	0.0000145	0.65	0.00059
0.0007	0.000013	0.16	0.00058
0.0008	0.0002888	0.18	0.002727
0.0009	0.0008358	0.19	0.004776
0.0010	0.001565	0.21	0.006693
0.0011	0.002437	0.23	0.008523
0.0012	0.0034	0.24	0.01024
0.0013	0.004445	0.26	0.01189
0.0014	0.00552	0.28	0.01341
0.0015	0.006688	0.29	0.0150
0.0016	0.007864	0.31	0.01636
0.0017	0.00906	0.32	0.0177
0.0018	0.01028	0.34	0.01903
0.0019	0.01149	0.35	0.02024
0.0020	0.01272	0.36	0.02147
0.0021	0.0139	0.37	0.0229
0.0022	0.01523	0.39	0.02373
0.0023	0.01647	0.40	0.02483
0.0024	0.01770	0.41[a]	0.02586
0.0025	0.01894	0.42[a]	0.0269
0.0026	0.02017	0.43[a]	0.0278
0.0027	0.009136	0.78	0.01686
0.0028	0.00756	0.76	0.0150
0.0029	0.006222	0.75	0.01332
0.0030	0.00508	0.75	0.01181
0.0031	0.00411	0.74	0.01042
0.0032	0.00329	0.73	0.0092
0.0033	0.00258	0.73	0.0080
0.0034	0.001987	0.73	0.0069
0.0035	0.001495	0.72	0.00593
0.0036	0.001083	0.72	0.00498
0.0037	0.0007523	0.72	0.00410
0.0038	0.0004877	0.72	0.00326
0.0039	0.0002912	0.72	0.00249
0.0040	0.0001432	0.72	0.00173
0.0041	0.0000610	0.72	0.00102
0.0042	0.00000607	0.72	0.000349

[a] This is not the parameter for the tangency point but for a maximum. The curve is broken and the other maximum is positive for $z \simeq 0.85$ (see Fig. 5.9).

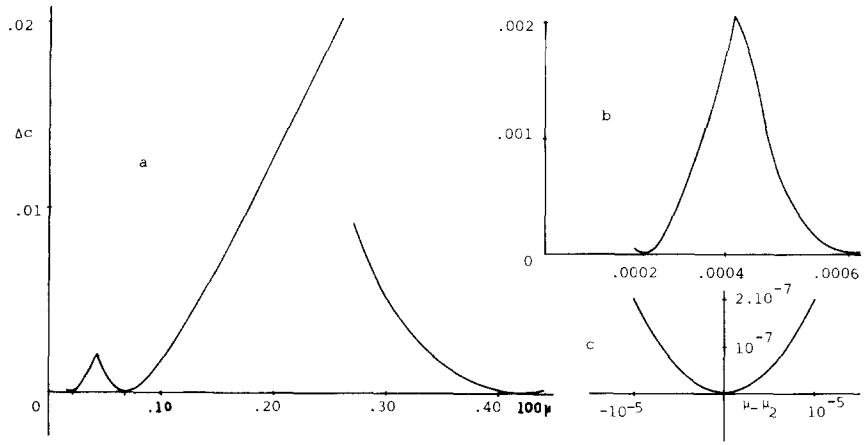

FIG. 5.6. Values of $(\mu, \Delta C)$ for which the first tangential homoclinic points are found.

A graphical representation of those values is given in Fig. 5.6a. The results show that there are (1, 1)-h.o. for values of μ sufficiently small provided we take suitable values of ΔC above $\Delta C(\mu)$. An enlargement of $\Delta C = \Delta C(\mu)$ for $\mu \in [\mu_4, \mu_3]$ is given in Fig. 5.6b. The values near one of the zeros, μ_2, are displayed with a larger magnification in Fig. 5.6c. Values of $\Delta C(\mu)$ for μ near μ_2 are given in Table III. The value of the parameter z for which the tangency occurs is also given in Table II. Furthermore if $(x_{\text{p.o.}}, 0, 0, \dot{y}_{\text{p.o.}})$, $\dot{y}_{\text{p.o.}} > 0$, are initial conditions for the p.o. of the family (c) for a given μ and $\Delta C = \Delta C(\mu)$, the value of $D = x_{L_2} - x_{\text{p.o.}}$ is also displayed in the same table.

The values of $\Delta C(\mu)$ shown in Fig. 5.6 need several comments. As follows

TABLE III

Values of ΔC for μ near μ_2 Related to Tangential (1, 1)-h.o.

$10^6 \Delta\mu^a$	$10^8 \Delta C$	$10^6 D$	$10^6 \Delta\mu$	$10^8 \Delta C$	$10^6 D$
3	2.2	21	−3	1.9	19
4	3.3	25	−4	3.3	26
5	5.2	32	−5	5.2	32
6	7.4	39	−6	7.4	38
7	10.0	45	−7	10.1	45
8	13.2	51	−8	13.2	51
9	16.6	58	−9	16.7	58
10	20.5	64	−10	20.6	64

[a] $\Delta\mu = \mu - \mu_2$.

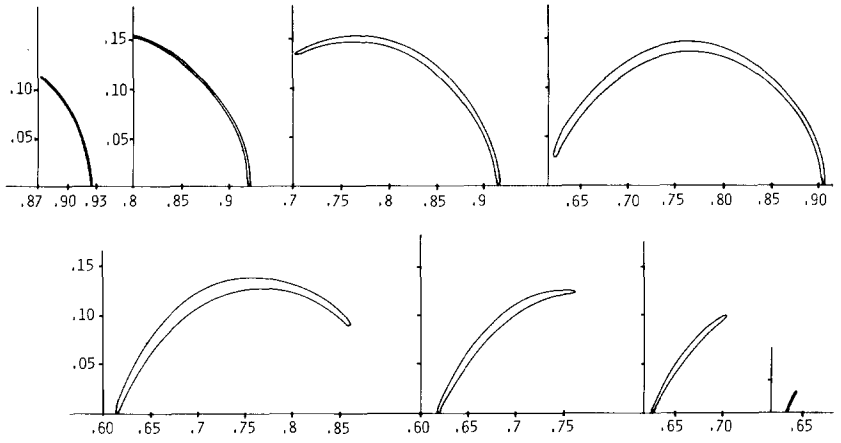

FIG. 5.7. Evolution of the section of $W^{u,S}_{\text{p.o.}}$ with $y=0$, $x>0$, producing tangential h.o. between μ_4 and μ_3. Values of $10^5\mu$: 23, 25, 30, 40, 45, 50, 55, 65.

from Section 4 (or from Fig. 5.5) for $\mu \in (\mu_4, \mu_3)$ and $\Delta C = \Delta C(\mu)$, the curve $\Gamma_1^{u,S}$ remains in the upper part of the $(x, \dot{x})$ plane. Going from μ_4 to μ_3, $\Gamma_1^{u,S}$ suffers some transformations. First, it becomes larger, and after some bending appears, displaying two minima. We remember that due to the tangency the absolute minimum is kept to zero. For some value $\mu = \hat{\mu}_3$ the two minima are equal. After that there is an exchange of the minima, the bending disappears and the curve reduces to one point for $\mu = \mu_3$. Figure 5.7 shows the evolution. The prevalence of one or of the other minima explains the lack of continuity of $(d/d\mu)\,\Delta C(\mu)$ observed in Fig. 5.6b. Qualitatively we can hope that in the (μ_3, μ_2) range the behavior of $\Delta C(\mu)$ remembers the one observed in (μ_4, μ_3). However, there is a difficulty. Up to the present we have forgotten that for values of $(\mu, \Delta C(\mu))$ we can escape from McGehee's region. Therefore we cannot assure that orbits on $W^{u,S}_{\text{p.o.}}$ possess no loops when projected in $\bar{N}_{\text{far}}$. In fact they exist and for $\mu = 0.0024$, $\Delta C = 0.0177$ the projections of different orbits on $W^{u,S}_{\text{p.o.}}$ are qualitatively given in Fig. 5.8 for some values of the parameter z: 0.816, 0.833, 0.85, 0.866, 0.883, 0.9, 0.916. This evolution of the loops shows that one plane $y=0$ cannot be taken as a global surface of section for the Poincaré map if we want to produce $\Gamma_1^{u,S}$ diffeomorphic to S^1. At any rates, if the first intersection in $\bar{N}_{\text{far}}$ is taken the continuity is lost and $\Gamma_1^{u,S}$ is broken. In Fig. 5.9 the evolution of $\Gamma_1^{u,S}$ for $\mu \in (\mu_3, \mu_2)$ and $\Delta C = \Delta C(\mu)$ is given, including the broken curves.

Several computations have been done concerning the Jupiter region.

First of all we compute invariant manifolds for Hill's equations. We recall (see [15] and Section 4) that for the equations $\ddot{x} - 2\dot{y} =$

$3x - x(x^2+y^2)^{-3/2}$, $\ddot{y} + 2\dot{x} = -y(x^2+y^2)^{-3/2}$ the critical points are $x = \pm 3^{-1/3}$, $y = 0$ and the z.v.c. for that level of the Jacobi constant ($C = 3^{4/3}$) has two asymptotes at $x = \pm 3^{1/6}$. Left and right branches, $W^{u,H}_{L_2,-}$, $W^{u,H}_{L_2,+}$, of the unstable manifold are therefore essentially different. The first one remains in a bounded region and wraps around the infinitesimal primary. The motion is far from being integrable. No

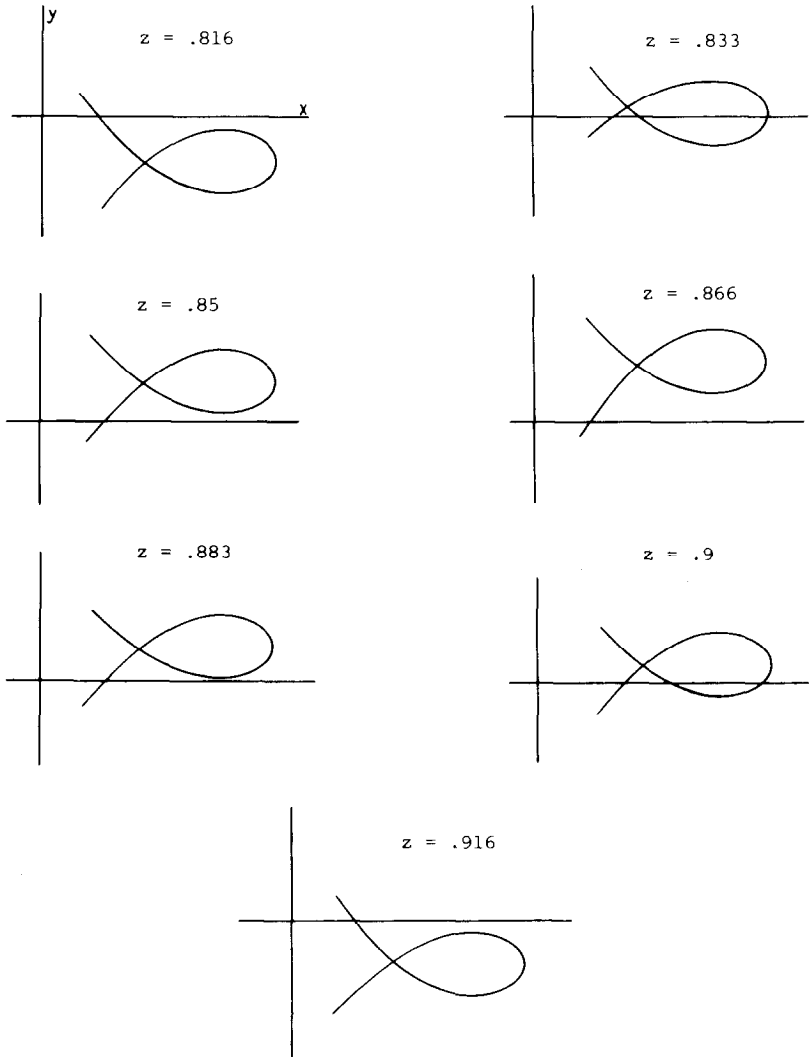

FIG. 5.8. Qualitative picture of several orbits belonging to $W^{u,S}_{\text{p.o.}}$ for $\mu = 0.0024$, $\Delta C = 0.0177$ displaying changes in the number of cuts with $y = 0$.

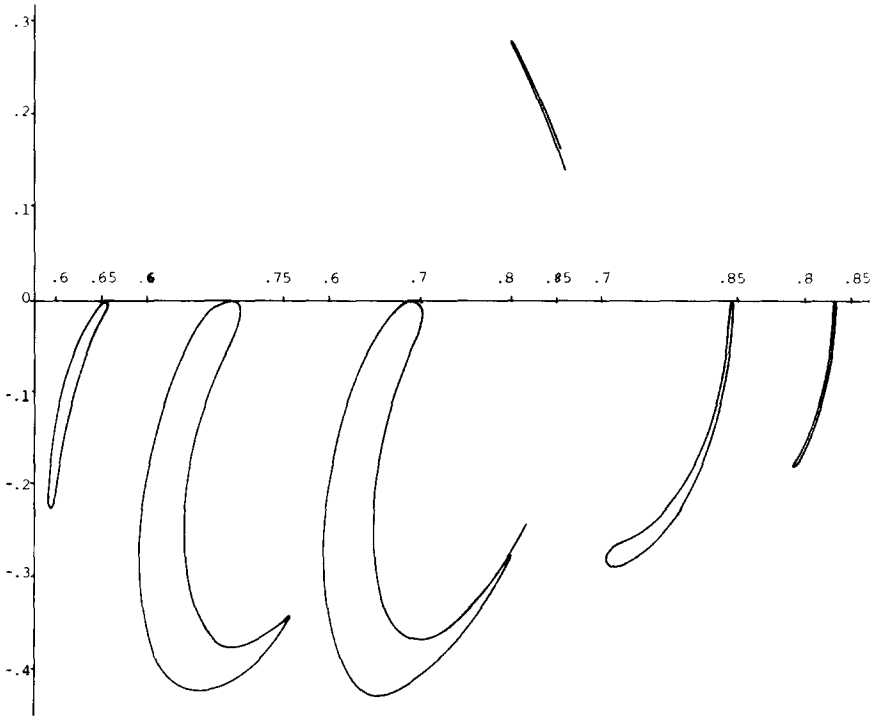

FIG. 5.9. Evolution of the section of $W^{u,S}_{\text{p.o.}}$ with $y=0$, $x>0$, for $\mu \in [\mu_3, \mu_2]$. Values of $10^4\mu$: 10, 22, 24($\Delta C = 0.0177$), 35, 40.

integrable hamiltonian can be taken as a reference to get properties of Hill's motion. The first 100 intersections of $W^{u,H}_{L_2,-}$ with the plane $y=0$ were computed. Some of them are given in Table IV. If for some cut we get $\dot{x}=0$ then $W^{u,H}_{L_2,-}$ would be a homoclinic orbit. We note that for the 46th cut $|\dot{x}|$ is small, but definitely not zero. We conjecture that $W^{u,H}_{L_2,-}$ is not a homoclinic orbit but, however, there is no lower bound of the values of $|\dot{x}|$ at the intersection. For $W^{u,H}_{L_2,+}$ we get an unbounded manifold as has been described in Section 4. The first 100 intersections with $\dot{x}=0$ were computed and they are partially given in Table IV. Some numerical fits obtained from these intersections are:

$$t_k = 6.009087 + k\pi + (-1)^{k+1} 0.00359\, k^{-2},$$

$$x_k = 1.30722979 - 0.0119628/(k/2) \text{ for } k \text{ even},$$

$$x_u = 5.573347145 - 0.0119628/(k/2) \text{ for } k \text{ odd},$$

giving in the limit ($k \to \infty$),

$x = \alpha + \beta \cos(t - t_0)$, $y = \gamma - t\frac{3}{2}\alpha - 2\beta \sin(t - t_0)$ with
$\alpha = 3.4402885$, $\beta = 2.133059$,

$t_0 = 2.86749$, $\gamma = 31.719$ (the coefficient of t obtained independently is 5.1604325).

The plots of $W^{u,H}_{L_2}$ are presented in Fig. 5.10.

From the first cut in the inner part we can obtain the limiting value $\tan \alpha(1)$ given in Table I.

For $\Delta C = 10^{-7}$ Hill's equations have a small p.o. in place of L_2. Figure 5.11 offers again the left and right branches $W^{u,H}_{\text{p.o.},-}$, $W^{u,H}_{\text{p.o.},+}$ of the corresponding unstable invariant manifold. They are cut by $y = 0$ (for the inner part) and for the values of y such that $W^{u,H}_{L_2,+}$ has $\dot{x} = 0$ (for the outer part). The first eight intersections are given in each case. For the outer part we can check the behavior predicted in Section 4, finding a very good agreement.

Finally, we return to the restricted three-body problem thought of as a perturbation of Hill's problem in order to describe what happens in the J region. If μ and ΔC are small enough we can hope that only small variations with respect to Hill's behavior will be found. For instance, for

TABLE IV

Several Cuts of $W^{u,H}_{L_2}$

	Inner part (cuts with $y = 0$)			Outer part (cuts with $\dot{x} = 0$)		
k	t^a	x	$\dot{x}$	t^a	x	y
1	6.120919	−0.08272859	−0.60600631	9.152296	5.55296845	−16.144853
2	7.018772	0.38064034	−0.44664138	12.291128	1.29529919	−32.264984
3	7.499447	−0.24850624	−0.48125251	15.434104	5.56555896	−48.437216
4	8.275218	0.20091020	−0.51922112	18.575158	1.30124073	−64.613838
5	8.763175	−0.43413008	−0.44083159	21.717140	5.56859888	−80.802459
6	9.790373	0.05143564	−0.40064716	24.858509	1.30323596	−96.992652
7	11.116769	−0.56869695	0.19522501	28.000282	5.56994049	−113.188102
8	11.862340	0.12473874	0.36913580	31.141753	1.30423481	−129.384355
9	12.701590	−0.40073660	0.24930374	34.283449	5.57069299	−145.583549
10	13.298910	0.24065002	0.25990923	37.424965	1.30483424	−161.783227
⋮						
46	40.597763	0.24831566	−0.00061750	150.522347	1.30670961	−745.242440
⋮						
98	80.604914	0.59414423	0.15907706	313.885167	1.30698565	−1588.179998
99	82.045551	−0.05458986	−0.55441304	317.026760	5.57310546	−1604.390835
100	83.029657	0.40533524	−0.49796874	320.168352	1.30699053	−1620.601675

[a] From an arbitrary origin taken on the unstable manifold $W^u_{L_2}$ (Hill problem).

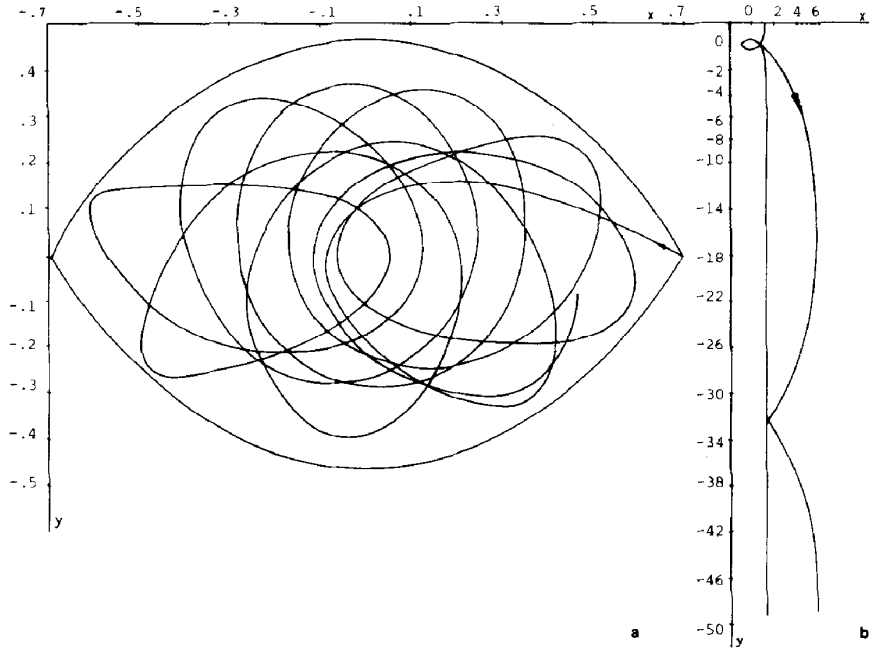

FIG. 5.10. Projection on the (x, y) plane of $W^{u,H}_{L_2}$: (a) left branch (inner branch); (b) right branch (outer branch).

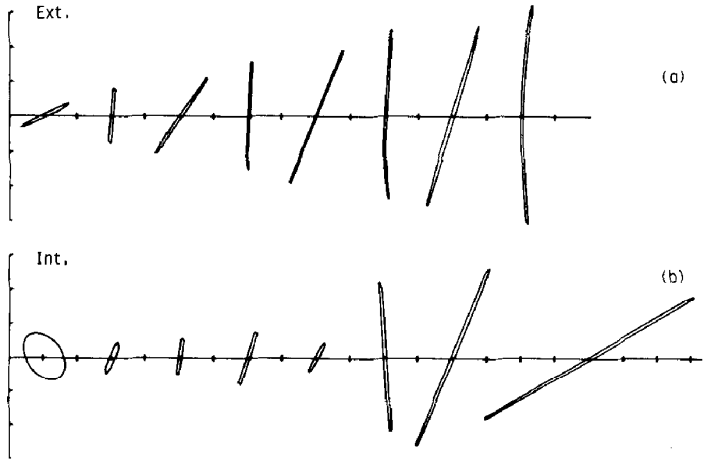

FIG. 5.11. Sections of $W^{u,H}_{\text{p.o.}}$ for $\Delta C^H = 10^{-7}$: (a) right branch for values of y for which $W^{u,H}_{L_2}$ has extrema in the x variable; (b) left branch for $y = 0$. The plots are made taking as origin the corresponding intersections for $W^{u,H}_{L_2}$. Scale: Each division is of length 10^{-3} except for the even plots in (a) where in the x axis each division is of length 10^{-2}.

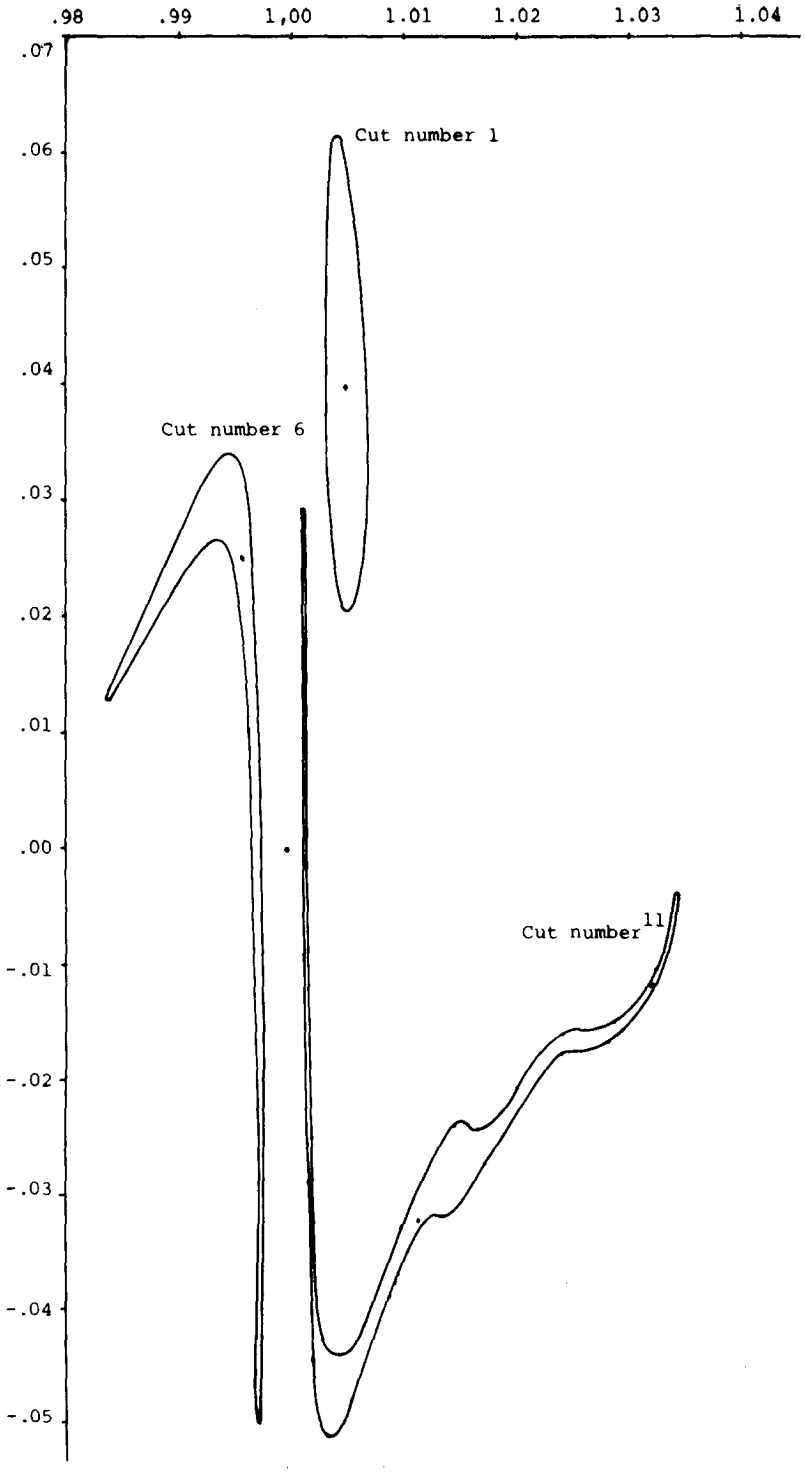

FIG. 5.12. Section numbers 1, 6, 11 of $W^{u,J}_{\text{p.o.}}$ with $y=0$ for $\mu=0.00025$, $C=0.0000783$.

$\mu = 0$, $\Delta C = 0$ the 46th cut of $W^{u,H}_{L_2,-}$ is near zero. Small variations in ΔC shall produce a curve cutting the axis x and so giving homoclinic points (indeed (46,46) ones). For μ small enough this property will be preserved.

A different approach has been undertaken. Being interested in values for which homoclinic points exist in the J region we merely took $\mu = 0.00025$, $\Delta C = 0.0000783$ and proceeded with the intersections of $W^{u,J}_{\text{p.o.},-}$ with $y = 0$. The cut numbers 1, 6, 11 are given in Fig. 5.12 (in fact the 4th cut already meets the x axis), so getting homoclinic points in the J region. For those values of μ, ΔC Theorem C will be applicable.

Finally, as a complementary check of formulas (4.16) and (4.17) and the expressions Δ_e, Δ_o given in Section 4, Fig. 5.13 shows $W^{u,S}_{\text{p.o.}} \cap \{y = 0, x > 0\}$ for the pairs of $(\mu, \Delta C)$ given by $(10^{-4}, 10^{-3})$, $(10^{-6}, 10^{-5})$, $(10^{-8}, 10^{-6})$, showing a good agreement with predictions.

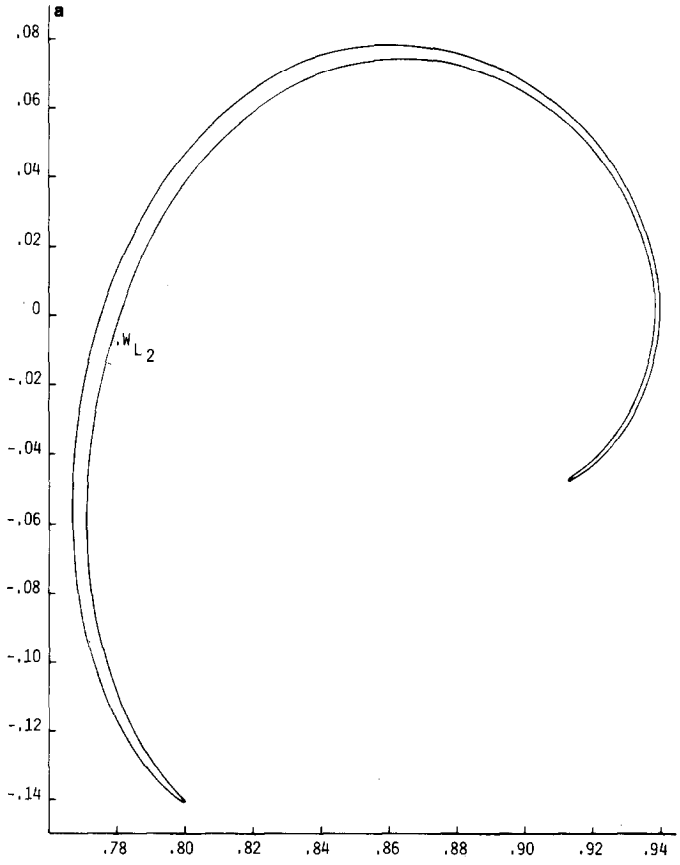

FIG. 5.13. Sections of $W^{u,S}_{\text{p.o.}}$ with $y = 0$, $x > 0$. Values of $(\mu, \Delta C)$: (a) $(10^{-4}, 10^{-3})$; (b) $(10^{-6}, 10^{-5})$; (c) $(10^{-8}, 10^{-6})$.

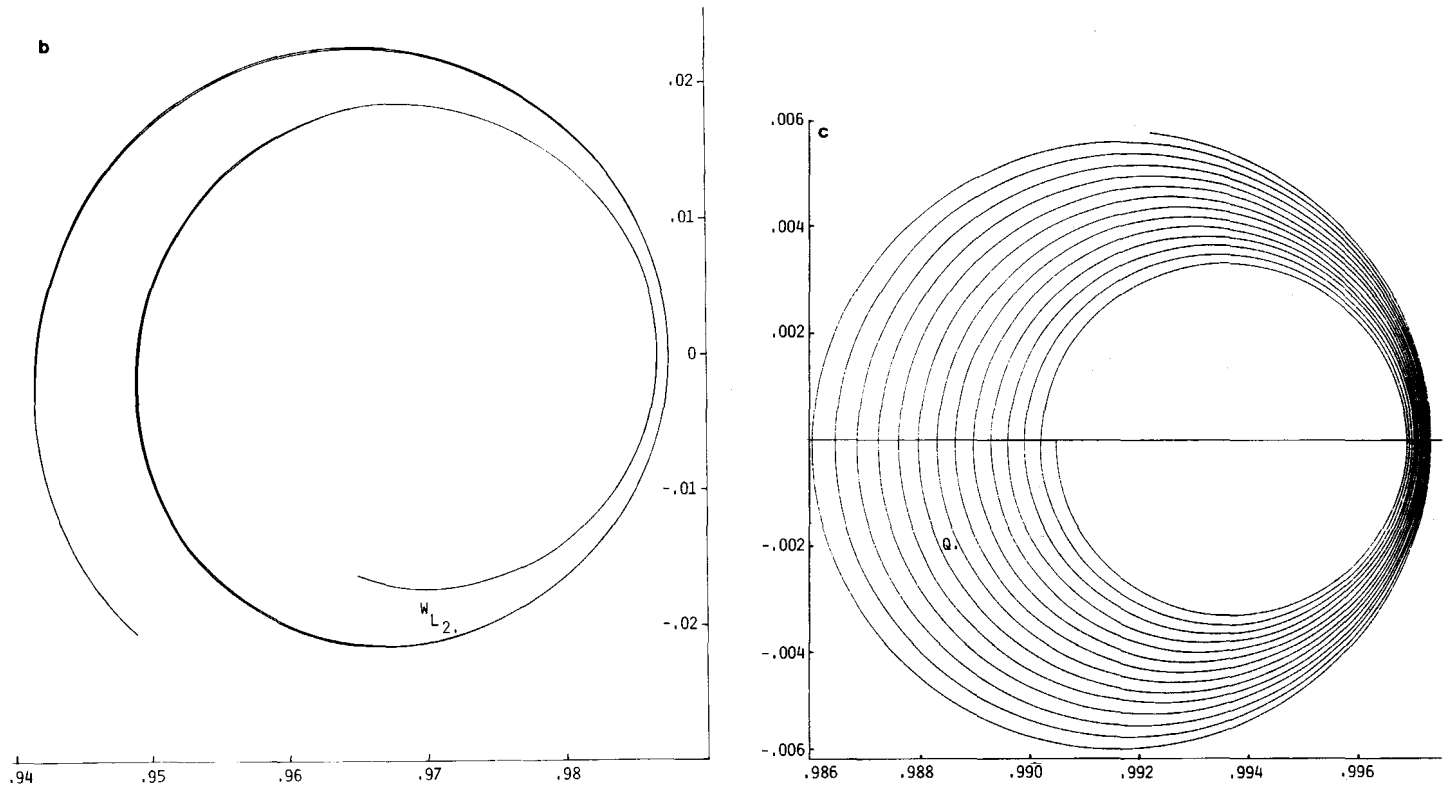

FIG. 5.13—*Continued.*

Concerning the values k_1, k_2, τ from Section 4 they can be roughly obtained from Fig. 5.11 and the approximated values are $k_1 = 0.22$, $k_2 = 2.2$, $\tau = \pi$. From this we can estimate the value of L in (4.18) which agrees with the numerical results displayed in Fig. 5.6.

6. A Symbolic Dynamics Theorem and Its Consequences

Several problems in dynamics, reduced to the study of a two-dimensional diffeomorphism $\bar{T}$, have a fixed hyperbolic point p which possesses transversal homoclinic points associated to it. Let Q be a small set diffeomorphic to a square which is near a homoclinic point (see Fig. 6.1).

Consider the first return map T to Q induced by $\bar{T}$. It is defined on a subset of Q. The map T has a nice symbolic dynamics and it can be proved [12] that it has the Bernoulli shift as a subsystem. The alphabet of the doubly infinite sequences is the set of the natural numbers. In our situation more than that can actually be proved because we have the situation described in Fig. 6.2, that is, each one of the two branches W^u_+, W^u_- of the unstable manifold of the hyperbolic point meets transversally the corresponding branches of the stable one. Instead of a square Q now we have two big squares $\mathscr{U}_+, \mathscr{U}_-$. We can again study the first return map T from $\mathscr{U} = \mathscr{U}_+ \cap \mathscr{U}_-$ into itself. Note that, in particular, T or T^{-1} is not defined on the points of $\mathscr{U}$ belonging to the invariant manifolds of p. We have a kind of singular Poincaré map as it has been considered by Devaney [5] and therefore we must consider in fact eight small squares. What can be found as a subsystem of T is now a shift based on $\mathbb{Z}$ instead of $\mathbb{N}$, the changes of sign allowing for changes from $\mathscr{U}_+$ to $\mathscr{U}_-$ or vice versa.

Let $\mathscr{A}$, $\mathscr{B}$, $\mathscr{C}$, $\mathscr{D}$, $\mathscr{E}$, $\mathscr{F}$, $\mathscr{G}$ and $\mathscr{H}$ be the rectangles $(-1.5, -1) \times (-0.5, 0.5)$, $(-1, -0.5) \times (-0.5, 0.5)$, $(-1.5, -0.5) \times (0, 0.5)$, $(-1.5, -0.5) \times (-0.5, 0)$, $(0.5, 1.5) \times (-0.5, 0)$, $(0.5, 1.5) \times (0, 0.5)$, $(0.5, 1) \times (-0,5, 5)$ and $(1, 1.5) \times (-0.5, 0.5)$, respectively (see Fig. 6.3). Let $\mathscr{U}_- = (\mathscr{A} \cup \mathscr{B}) \cap (\mathscr{C} \cup \mathscr{D})$, $\mathscr{U}_+ = (\mathscr{G} \cup \mathscr{H}) \cap (\mathscr{E} \cup \mathscr{F})$ and $\mathscr{U} = \mathscr{U}_- \cup \mathscr{U}_+$. Let $r \in (0, \frac{1}{2})$. We define a vertical curve in $\mathscr{A}$ as a lipschitzian function $x = v(y)$ with Lipschitz constant equal to r, where $y \in (-0.5, 0.5)$. A vertical strip in $\mathscr{A}$

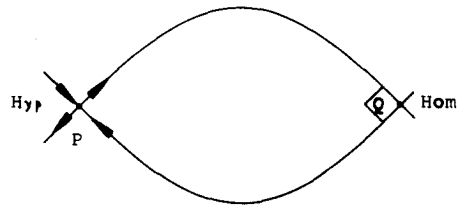

FIG. 6.1. Transversal homoclinic point for a diffeomorphism.

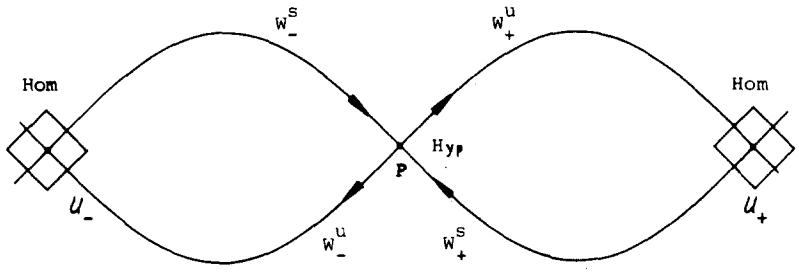

FIG. 6.2. Two nonrelated transversal homoclinic points associated to a saddle.

limited by the two vertical curves v_1, v_2 is the set $V = \{(x, y) \in \mathscr{A} | v_1(y) \leqslant x \leqslant v_2(y)\}$. The diameter of V is defined as $d(V) = \max_{y \in (0.5,0.5)} (v_2(y) - v_1(y))$. In a similar way vertical curves and strips in $\mathscr{B}$, $\mathscr{G}$, $\mathscr{H}$ and horizontal curves and strips in $\mathscr{C}$, $\mathscr{D}$, $\mathscr{E}$, $\mathscr{F}$ can be defined.

PROPOSITION 6.1 (Moser [12]). (1) *Let $V_1 > V_2 > V_3 \cdots$ be a sequence of vertical strips such that $d(V_k) \to 0$ when $k \to \infty$. Then $\bigcap_{k=1}^{\infty} V_k$ is a vertical curve. This holds for horizontal strips mutatis mutandis.*

(2) *Any horizontal curve and any vertical curve in $\bar{\mathscr{U}}_-$ or $\bar{\mathscr{U}}_+$ intersect exactly at one point.*

Let $\mathscr{T}$ be a homeomorphism from $\mathscr{U}$ into $\mathscr{T}(\mathscr{U}) \subset \mathbb{R}^2$ such that:

(a) There are four families of pairwise disjoint vertical strips $V\mathscr{A}_n$, $V\mathscr{B}_n$, $V\mathscr{G}_n$, $V\mathscr{H}_n$, $n = 1, 2, 3,...$, and four families of pairwise disjoint horizontal strips $H\mathscr{C}_n$, $H\mathscr{D}_n$, $H\mathscr{E}_n$, $H\mathscr{F}_n$, $n = 1, 2, 3,...$, such that $\mathscr{T}(V\mathscr{A}_n) = H\mathscr{E}_n$, $\mathscr{T}(V\mathscr{B}_n) = H\mathscr{C}_n$, $\mathscr{T}(V\mathscr{G}_n) = H\mathscr{F}_n$, $\mathscr{T}(V\mathscr{H}_n) = H\mathscr{D}_n$, $n = 1, 2, 3,...$.

The horizontal (resp. vertical) boundaries of the horizontal strips are the images under $\mathscr{T}$ of the horizontal (resp. vertical) boundaries of the corresponding vertical strip.

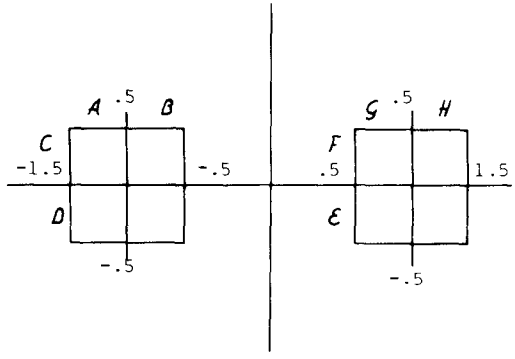

FIG. 6.3. The model based on several squares.

Furthermore the strips are ordered in such a way that for horizontal strips the index increases when the strips approach the x axis and for vertical strips when they approach the lines $x=-1$ (in $\mathscr{A}, \mathscr{B}$) or $x=1$ (in $\mathscr{G}, \mathscr{H}$). The set of horizontal strips is completed by adding $H\mathscr{C}_\infty = H\mathscr{D}_\infty = (-1.5, -0.5)\times\{0\}$ and $H\mathscr{F}_\infty = H\mathscr{E}_\infty = (0.5, 1.5)\times\{0\}$. Limit sets $V\mathscr{A}_\infty = V\mathscr{B}_\infty$ and $V\mathscr{G}_\infty = V\mathscr{H}_\infty$ are also introduced. We require that $V\mathscr{A}_n$ tends to $V\mathscr{A}_\infty$ when $n\to\infty$ and that a similar condition be satisfied for the other seven families of strips.

(b) Let $V\subset\bigcup_n V\mathscr{A}_n$ be a vertical strip. Then $V'_n = \mathscr{T}^{-1}(V)\cap V\mathscr{B}_n$ and $V''_n = \mathscr{T}^{-1}(V)\cap V\mathscr{H}_n$ are two vertical strips for all n, and for some $s\in(0,\frac{1}{2})$ we have that $d(V'_n)\leqslant s\cdot d(V)$, $d(V''_n)\leqslant s\cdot d(V)$. Let $H\subset\bigcup_n H\mathscr{C}_n$ be a horizontal strip. Then $H'_n = \mathscr{T}(H)\cap H\mathscr{E}_n$ and $H''_n = \mathscr{T}(H)\cap H\mathscr{C}_n$ are two horizontal strips for all n and we have also $d(H'_n)\leqslant s\cdot d(H)$, $d(H''_n)\leqslant s\cdot d(H)$. Similar assertions are true for the other families of vertical and horizontal strips.

Let $\Sigma = \{a=(a_j),\ j\in\mathbb{Z},\ a_j\in\mathbb{Z}-\{0\},\ \forall j\}$ the set of doubly infinite sequences of elements of $\mathbb{Z}-\{0\}$. Σ can be topologized with the product topology obtained from the discrete one in $\mathbb{Z}-\{0\}$. A compactification $\bar{\Sigma}$ of Σ is obtained with the inclusion of the sequences of the types

$$\beta\colon (a_k, a_{k+1},\ldots, a_q,\ldots)\ k\leqslant 0, \qquad a_k=\infty,\ a_n\in\mathbb{Z}-\{0\},\ \forall n>k,$$

$$\gamma\colon (\ldots, a_k,\ldots, a_{q-1}, a_q)\ q>0, \qquad a_q=\infty,\ a_n\in\mathbb{Z}-\{0\},\ \forall_n<q,$$

$$\delta\colon (a_k,\ldots, a_q)\ k\leqslant 0,\ q>0, \qquad a_k=a_q=\infty,\ a_n\in\mathbb{Z}-\{0\},\ \forall_n\in(k,q)\cap\mathbb{Z},$$

and we call type α the elements of $\bar{\Sigma}$ being in Σ.

A base of neighborhoods in $\bar{\Sigma}$ is defined by

$$W_j(a) = \{a'\in\bar{\Sigma} | a'_n = a_n \text{ if } |n|\leqslant j\}, \qquad j=1, 2, 3,\ldots \text{ if } a \text{ is of type } \alpha,$$

$$W_j(a) = \{a'\in\bar{\Sigma} | a'_n = a_n \text{ if } k<n\leqslant j \text{ and } a'_k\geqslant j\}, \quad j=1, 2, 3,\ldots \text{ if } a \text{ is of type } \beta,$$

and similar definitions for type γ and δ elements.

On Σ we define the Bernoulli shift σ through $(\sigma(a))_j = a_{j-1}$, $\forall j\in\mathbb{Z}$, $a\in\Sigma$. This map can be extended to a map $\bar{\sigma}$ from $\bar{\Sigma}$ to $\bar{\Sigma}$ in the natural way. The domain of definition is then $D(\bar{\sigma}) = \{a\in\bar{\Sigma} | a_0\neq\infty\}$ and the range is $R(\bar{\sigma}) = \{a\in\bar{\Sigma} | a_{-1}\neq\infty\}$. We say that $\bar{\sigma}$ is a subsystem of $\mathscr{T}$ if there is a homeomorphism h from $\bar{\Sigma}$ to $h(\bar{\Sigma})\subset\mathscr{U}$ such that $h\circ\bar{\sigma} = \mathscr{T}\circ h|_{D(\bar{\sigma})}$.

THEOREM 6.1. *Let $\mathscr{T}:\mathscr{U}\to\mathbb{R}^2$ be a map satisfying the preceding conditions* (a) *and* (b). *Then $\mathscr{T}$ has two copies of the shift $\bar{\sigma}$ as a subsystem.*

Proof. First we construct the homeomorphism h. The fact that there are two copies means that given an element $a\in\bar{\Sigma}$ we can define one point in $\mathscr{U}_-$ and one point in $\mathscr{U}_+$ as images of a under h. We call them $h_-(a)$,

$h_+(a)$, respectively. The construction of h_+ being symmetrical of the construction of h_-, we present only the last one. In $\bar{\Sigma}$ we have four types of elements $\alpha, \beta, \gamma, \delta$. We give explicitly the images for elements of types α, β, the ones for types γ, δ being similar.

Let $a = (..., a_{-2}, a_{-1}, a_0, a_1, a_2, ...)$ an element of type α. We shall show that there is a unique point $p \in \mathscr{U}_-$ such that for all $m \in \mathbb{Z}$, $\mathscr{T}^{-m}(p)$ belongs to one of the two vertical strips with label $|a_m|$ contained in $\mathscr{U}_-$ or $\mathscr{U}_+$, according to $\prod_j a_j$ being positive or negative, where j ranges over the set of integers contained in the convex envelope $\langle 0.5, m+0.5 \rangle$. We define $h_-(a)$ as the point p.

Note that for elements a of type α all the successive images and preimages of $h_-(a)$ or $h_+(a)$ under $\mathscr{T}$ exist. However, for an element b of type β, $b = (b_k, b_{k+1}, ..., b_q, ...)$, all the preimages exist but only the $|k|$ first images do. That is, $\mathscr{T}^{|k|}h(b)$ belongs to a vertical strip with index equal to ∞.

One checks immediately that $\mathscr{T}$ (resp. $\mathscr{T}^{-1}$) applied to each one of the eight small squares $\mathscr{C} \cap \mathscr{A}$, $\mathscr{C} \cap \mathscr{B}$, $\mathscr{D} \cap \mathscr{A}$, $\mathscr{D} \cap \mathscr{B}$, $\mathscr{F} \cap \mathscr{G}$, $\mathscr{F} \cap \mathscr{H}$, $\mathscr{E} \cap \mathscr{G}$, $\mathscr{E} \cap \mathscr{H}$ produces horizontal strips in $\mathscr{E}$, $\mathscr{C}$, $\mathscr{E}$, $\mathscr{C}$, $\mathscr{F}$, $\mathscr{D}$, $\mathscr{F}$, $\mathscr{D}$ (resp. vertical strips in $\mathscr{B}$, $\mathscr{B}$, $\mathscr{H}$, $\mathscr{H}$, $\mathscr{G}$, $\mathscr{G}$, $\mathscr{A}$, $\mathscr{A}$). We use the notation $\mathscr{T}_{|n|}$ (resp. $\mathscr{T}_{|n|}^{-1}$) applied to some vertical (resp. horizontal) strip as the part of the image (resp. preimage) contained in the two corresponding horizontal (resp. vertical) strips with label $|n|$.

Given $a \in \Sigma$ we define one vertical and one horizontal curve, V and H, in $\mathscr{U}_-$ through the relations

$$V = \mathscr{T}_{|a_0|}^{-1}(\mathscr{M}_{i_0} \cap \mathscr{T}_{|a_{-1}|}^{-1}(\mathscr{M}_{i_{-1}} \cap \mathscr{T}_{|a_{-2}|}^{-1}(\mathscr{M}_{i_{-2}} \cdots))),$$

where $\mathscr{M}_1 = \mathscr{C}$, $\mathscr{M}_2 = \mathscr{F}$, $\mathscr{M}_3 = \mathscr{E}$, $\mathscr{M}_4 = \mathscr{D}$, being $i_j = 2 - \operatorname{sign}(a_j) + [1 - \operatorname{sign}(\prod_{i=j+1}^{0} a_i)]/2$, $j \leqslant 0$, and

$$H = \mathscr{T}_{|a_1|}(\mathscr{N}_{i_1} \cap \mathscr{T}_{|a_2|}(\mathscr{N}_{i_2} \cap \mathscr{T}_{|a_3|}(\mathscr{N}_{i_3} \cdots))),$$

where $\mathscr{N}_1 = \mathscr{B}$, $\mathscr{N}_2 = \mathscr{G}$, $\mathscr{N}_3 = \mathscr{H}$, $\mathscr{N}_4 = \mathscr{A}$, being

$$i_j = 2 - \operatorname{sign}(a_j) + \left[1 - \operatorname{sign}\left(\prod_{i=1}^{j-1} a_i\right)\right]/2, \qquad j > 0.$$

It is immediate, due to conditions (a) and (b), that taking a finite part in the expressions of V or H we get a vertical or horizontal strip. By the same condition (b), when the number of elements in a finite part increases, the diameter of the strips decreases going exponentially to zero and therefore V and H are curves by Proposition 6.1. They meet exactly in one point that we take as the point p. By the construction of V and H we obtain that $\mathscr{T}^{-m}(p)$ belongs to the suitable strips.

If b is of type β then $V = \mathscr{T}^{-1}_{|a_0|}(\mathscr{M}_{i_0} \cap \mathscr{T}^{-1}_{|a_{-1}|}(\mathscr{M}_{i_{-1}} \cap \cdots \mathscr{T}^{-1}_{|a_k|}(\mathscr{M}_{i_k}) \cdots))$ and this is clearly a vertical curve. Note that the possible ambiguity in the determination of $\mathscr{M}_{i_k}$ due to the two possible choices of the sign of ∞ is not a problem because in each one of the big squares there is only one vertical strip with label ∞.

The continuity of h (h_- or h_+) comes as follows:

Two close elements in $\bar{\Sigma}$ have a large number of coincident elements (or one of the elements is as large as we wish). Therefore the corresponding points p, p' belong to the same vertical and horizontal strips with diameters as small as desired if the elements are close enough.

The map is injective because strips of the same class with different labels are disjoint. This and the compacity of $\bar{\Sigma}$ ensures that $h_-(h_+)$ is a homeomorphism between $\bar{\Sigma}$ and their image.

The conjugacy with the shift, i.e., $h \circ \bar{\sigma} = \mathscr{T} \circ h_{D(\bar{\sigma})}$, follows from the construction. ∎

When the map $\mathscr{T}$ is of class $\mathscr{C}^1$, condition (b) is usually replaced by another condition, which is easier to check, that we formulate as condition (c). That (c) and (a) imply (b) is proved in [12].

Condition (c): There exists $R \in (0, \frac{1}{2})$ such that for the field of sectors S^+ defined at the points of coordinates (x, y) of vertical strips by

$$S^+(x, y) = \{(u, v) \in T_{(x,y)}\mathscr{U} \mid |v| \leqslant R|u|\},$$

$T_{(x,y)}\mathscr{U}$ being the tangent space to $\mathscr{U}$ at the point (x, y), the following assertions hold:

(I) S^+ is mapped into itself by the differential $D\mathscr{T}$.

(II) If $(u_0, v_0) \in S^+(x, y)$ and $(u_1, v_1) = D\mathscr{T}_{(x,y)}(u_0, v_0) \in T_{\mathscr{T}(x,y)}\mathscr{U}$, then $|u_1| \geqslant R^{-1}|u_0|$.

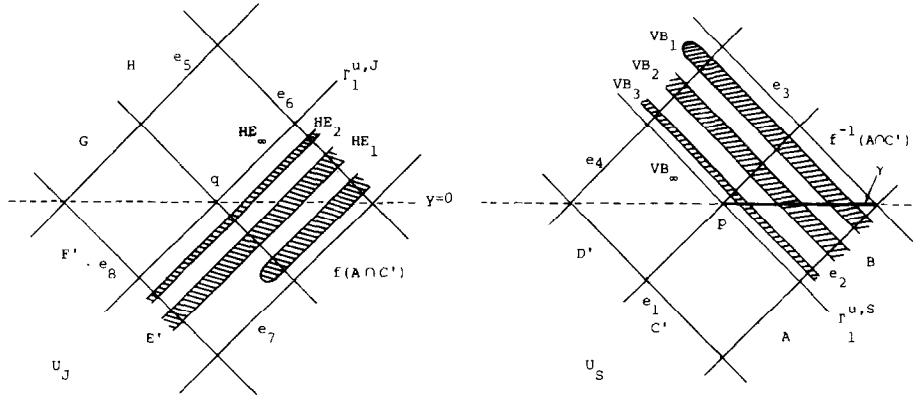

FIG. 6.4. The topological squares and the images of some strips.

In a similar way, if S^- is the field of sectors defined on points of the horizontal strips by $|u| \leqslant R|v|$, it is invariant by $D\mathscr{T}^{-1}$ and $|v_0| \geqslant R^{-1}|v_1|$.

In the sequel we shall apply Theorem 6.1 to our situation in the RTBP. Let U be the set defined on Section 3. It is bounded by eight differentiable arcs denoted by $e_1, e_2, \ldots, e_8$ (see Fig. 6.4).

It is clear that $sU = U$ where s is the symmetry on the $(x, \dot{x})$ plane (see Section 3). We remark that each one of the sets U_S, U_J whose union is U is diffeomorphic to an open square with two lines (parallel to the sides through the center) removed from the interior. U_S, U_J will play the role of $\mathscr{U}_-$, $\mathscr{U}_+$ (respectively) of the abstract theorem. The passage from U_S, U_J to $\mathscr{U}_-$, $\mathscr{U}_+$ will be given through a diffeomorphism. The sets A, B, C', D', E', F', G, H when intersected with U will play the role of $\mathscr{A}, \ldots, \mathscr{H}$.

Using the spiraling of the images of curves ending in $a^{\pm}_{1,2}$ (see last paragraph in Section 2) the image of $A \cap C'$ under f is a strip contained in E' of arbitrarily large length, cutting $\mathscr{U}$ an infinity of times and spiraling towards $\Gamma_1^{u,J}$, becoming narrower when approaching the limit. The intersection of this strip with $\mathscr{U}$ is formed by an infinity of components. All but perhaps one of the components are limited by the sides e_6 and e_8 (remember the first integrals are near L_2).

We call each of the components of $f(A \cap C') \cup U \subset E'$ a horizontal strip of E'. We only consider the horizontal strips of E' bounded by e_6 and e_8. In a similar way, $f(B \cap C')$, $f(A \cap D')$, $f(B \cap D')$, $f(G \cap F')$, $f(H \cap F')$, $f(G \cap E')$ and $f(H \cap E')$ define horizontal strips in C', E', C', F', D', F' and D', respectively.

We consider all the horizontal strips in E', i.e., the horizontal strips of $f(A \cap C')$ and those of $f(A \cap D')$. We denote these by $HE_1, HE_2, \ldots$, beginning with the strip nearest to e_7. Thus we have on E' a family of horizontal strips $\{HE_n\}$ bounded by the sides e_6, e_8 and such that its diameter tends to zero as n tends to infinity. We define $HE_\infty = \lim_{n \to \infty} HE_n$ (see Fig. 6.4). Similarly, we enumerate the horizontal strips on C', F' and D'.

An analogous study can be made to analyze $f^{-1}(A \cap C')$. Then $f^{-1}(A \cap C')$ is a strip contained in B of arbitrarily large length cutting U an infinity of times and spiraling towards $\Gamma_1^{u,S}$, becoming narrower when approaching the limit. The intersection of this strip with U is formed by an infinite number of components bounded by the sides e_4 and e_2. We call vertical strips of B to each one of the components of $f^{-1}(A \cap C') \cap U \subset B$. In a similar way $f^{-1}(B \cap C')$, $f^{-1}(A \cap D')$, $f^{-1}(B \cap D')$, $f^{-1}(G \cap F')$, $f^{-1}(H \cap F')$, $f^{-1}(G \cap E')$ and $f^{-1}(H \cap F')$ originate vertical strips in B, H, H, G, G, A and A, respectively.

We consider all the vertical strips of B, that is, the vertical strips of $f^{-1}(A \cap C')$ and the ones of $f^{-1}(B \cap C')$. We enumerate them beginning with the nearest one to e_3 by VB_1, $VB_2, \ldots$. Thus we have defined on B a family of vertical strips $\{VB_n\}$ bounded by the sides e_2, e_4 and such that its

diameter tends to zero as $n \to \infty$. We define $VB_\infty = \lim_{n\to\infty} VB_n$. Similarly, we enumerate the vertical strips on H, G, A.

LEMMA 6.1. *The following relations hold*:

$$f(VB_n) = HC_n, \qquad f(VG_n) = HF_n,$$
$$f(VH_n) = HD_n, \qquad f(VA_n) = HE_n.$$

Proof. We use essentially an argument of Moser [12]. From Lemma 3.1 we have

$$VB_n \subset s(fB \cap C') = sfB \cap B = f^{-1}sB \cap B = f^{-1}C' \cap B.$$

Therefore

$$f(VB_n) \subset C' \cap f(B) = \bigcup_{n=1}^{\infty} HC_n. \qquad (*)$$

In a similar way we have $f^{-1}(HC_n) = sfs(HC_n) = sf(VB_n) \subset s(\bigcup_{n=1}^{\infty} HC_n) = \bigcup_{n=1}^{\infty} VB_n$, and hence

$$HC_n = \bigcup_{n=1}^{\infty} f(VB_n). \qquad (**)$$

From (*), (**) it follows that $\bigcup_{n=1}^{\infty} f(VB_n) = \bigcup_{n=1}^{\infty} HC_n$.

As the strips of the type VB_n or HC_n are pairwise disconnected, each one of the strips VB_n must be sent by f onto one of the strips HC_m. It remains to show that $m = n$.

Let γ be the part of the $\dot{x} = 0$ axis contained in B (see Fig. 6.4). Under f the curve γ spirals in a way that $f\gamma \cap \gamma = \bigcup_{i=1}^{\infty} p_i$, where the points p_i are numbered on γ in a consistent way with the order in he $\dot{x} = 0$ axis. By Lemma 3.1 it follows that $f(\cup p_i) = \cup p_i$ and hence $f(p_i) = p_i$ follows because of the ordering. The points p_i are associated to symmetric p.o. (see later). As p_i belongs to a horizontal and to a vertical strip we get that the one is the image of the other, i.e., $m = n$, as desired. The remaining cases are proved mutatis mutandis. ∎

Now condition (a) follows essentially from Lemma 6.1. Condition (c) follows due to two facts. The first is that going from the spheres l_1, l_2 to the plane $(x, \dot{x})$ of the Poincaré map and the passage from U to $\mathcal{U}$ are diffeomorphisms. The second is that the flow in the inner part of the sphere is exactly given by the linear equations (see Section 2) in good coordinates, and condition (c) holds for this flow with a constant R as large as desired if U is sufficiently small. Therefore the shift of Theorem 6.1 is a subsystem of the Poincaré map f associated to the RTBP.

THEOREM C. *Consider a region S or J and an element $a \in \bar{\Sigma}$ such that $|a_j| > m = m(\mu, C)$ for all components of a. Then there are initial conditions (unique in a neighborhood of the homoclinic orbits associated to p and q) such that the orbit corresponding to such conditions enters the L region and leaves it going to the initial region or to the opposite according to whether m_0 is positive or not. The number of integer revolutions of the projection of the orbit on $R_b(\mu, C)$ around L_2 while the orbit remains in L is $|m_0|$. After that the same process begins again with m_1 in the place of m_0, m_2 in the place of m_1, etc. For negative time a similar behavior is described being $m_{-1}, m_{-2}, \ldots$ the associated integers. For this orbit the number of integer revolutions of the massless body around the Sun or Jupiter when the orbit is in the S or J region, respectively, is a constant depending on the region and on the selected homoclinic orbits. If a is of type β after $|k|$ steps the orbit tends asymptotically to the* p.o. *around L_2 without leaving L. If it is of type γ after l backwards steps it tends asymptotically to the* p.o. *remaining in L, and if it is of type δ after $|k|$ steps forward and l steps backwards it tends asymptotically to the* p.o. *without leaving L.*

Proof of Theorem C. Given a as in the statement of the theorem we define $a' \in \bar{\Sigma}$ such that $a' = a_n - m \cdot \operatorname{sign}(a_n)$. Then we apply Theorem 6.1. Let us suppose that we select initially the region U_S. Let z be equal to $h_-(a')$. (If we select U_J merely take $h_+(a')$.) Going from one vertical strip with label n to another with label $n+1$ means that the associated orbit has given one more revolution around L_2. The number m means the minimum number of integer revolutions around the p.o. given by the orbits associated to points in U before returning to U. We can adjust the size of U_S, U_J in order to get the same value of m for both parts.

Another problem where a theorem like Theorem C holds is the following. Consider the perturbed pendulum $\ddot{x} + \sin x = \varepsilon f(t)$ where f is an analytic T-periodic function with zero average. For ε small enough the invariant manifolds (stable and unstable) of the hyperbolic p.o. found near the point z ($x = \pi$, $\dot{x} = 0$) meet transversally (i.e., there are (1, 1)-transversal homoclinic orbits). Replacing the S and J regions of the RTBP by the libration and circulation regions and L by a neighborhood of the point z, Theorem C is true without any other change.

In some applications more than two regions of motion exist. Consider a hamiltonian system such that for a level $H = H_{\text{crit}}$ there are critical points $L_1, \ldots, L_n$, all of them of the saddle-center type and such that for $H \gtrsim H_{\text{crit}}$ there are infinitesimal periodic orbits. Suppose that for $H \lesssim H_{\text{crit}}$ the projection of the energy level on the configuration space has S connected components $\mathcal{R}_1, \ldots, \mathcal{R}_S$. The points L_i have one-dimensional stable and unstable invariant manifolds $W^{u,s}_{L_i}$ and the same is true (with dimension two) for the p.o. near L_i: $W^{u,s}_{\text{p.o.}i}$. We look at each point L_i as a couple of points L^*_{2i-1},

L_{2i}^* such that each one has only one branch of stable/unstable manifold (both branches leaving/entering the same $\mathscr{R}_k$ region). Geometrically $L_i = L_{2i-1}^* = L_{2i}^*$ but $W_{L_j^*}^u$ specifies the manifold and the branch. In a similar way we think in p.o.*i and $W_{\text{p.o.}*_i}^{u,s}$. A spherical annulus like the one obtained for the RTBP between l_1 and l_2 around L_i will be denoted by $\mathscr{L}_i$.

We define a relation R: We set iRj if $L_i^*, L_j^* \in \partial\mathscr{R}_k$ when $H = H_{\text{crit}}$ for some k and $W_{\text{p.o.}*_i}^u \cap W_{\text{p.o.}*_j}^s$ contains a heteroclinic orbit O_{ij} (homoclinic if $i=j$) fully contained in $\mathscr{L}_i \cup \mathscr{R}_k \cup \mathscr{L}_j$ for a level $H^* \gtrsim H_{\text{crit}}$, H^* fixed. Let $\zeta(p, q)$ be the function defined on $\mathbb{N} \times \mathbb{Z}$ through $\zeta(p, q) = p$ if $q > 0$, $\zeta(p, q) = p - (-1)^p$ if $q < 0$.

THEOREM 6.2. *Select a region $\mathscr{R}_k$ and a couple of sequences $(..., a_{-1}, a_0, a_1, a_2, ...)$, $(..., i_{-1}, i_0, i_1, i_2, ...)$ with $a_j \in \mathbb{Z}$, $|a_j| > m$, $1 \leqslant i_j \leqslant 2n$, $\zeta(i_j, a_j) Ri_{j+1}$ and $O_{\zeta(i_{-1}, a_{-1}), i_0} \subset \mathscr{L}_{\zeta(i_{-1}, a_{-1})} \cup \mathscr{R}_k \cup \mathscr{L}_{i_0}$, where m depends on the Hamiltonian and on the value H^*. Then there is an orbit starting in $\mathscr{R}_k$ such that gives $|a_0|$ revolutions around L_{i_0}, returns to $\mathscr{R}_k$ or escapes from it according to a_0 being positive or negative, then gives $|a_1|$ revolutions around L_{i_1}, etc. For backwards time there is a similar behavior. Extensions for sequences a of types β, γ, δ like in Theorem* 6.1 *are possible.*

As an example, for the Hénon–Heiles potential [2] there are four regions $\mathscr{R}$ (three of them unbounded) and three points L_i for $H = \frac{1}{6}$. Consider each L_i decoupled and the even points L_j^* the ones related to the bounded $\mathscr{R}$. Then pRq for $p, q \in \{2, 4, 6\}$. It is proved in [2] that none of the odd indexes can satisfy the relation R and that the even ones do for a suitable H^* (obtained numerically). In fact we believe this is true for all $H^* > \frac{1}{6}$. Then Theorem 6.2 applies. The same thing is true for examples with the hamiltonian $\frac{1}{2}(x^2 + y^2 + \dot{x}^2 + \dot{y}^2) + x^2y^2$.

Returning to the RTBP and $\mu = \mu_k$ (but this is true for general hamiltonians of two degrees of freedom having a center-saddle fixed point and an associated homoclinic orbit) a countable set of families of simple periodic orbits is found near the homoclinic one.

REFERENCES

1. V. M. ALEKSEEV, Quasirandom dynamical systems, I, II, III, *Math. USSR–Sb.* **5** (1968), 73–128; **6** (1968), 505–560; **7** (1969), 1–43.
2. R. C. CHURCHILL, G. PECELLI, AND D. L. ROD, A survey of the Hénon–Heiles Hamiltonian with applications to related examples, *in* "Lecture Notes in Physics Vol. 93," pp. 76–136, Springer–Verlag, New York/Berlin, 1978.
3. C. CONLEY, On the ultimate behavior of orbits with respect to an unstable critical point, *J. Differential Equations* **5** (1969), 136–158.
4. C. CONLEY, Twist mappings, analyticity and periodic solutions which pass close to an

unstable periodic solution, *in* "Topological Dynamics" (J. Auslander, Ed.), pp. 129–154, Benjamin, New York, 1968.
5. R. L. DEVANEY, Singularities in classical mechanical systems, *in* "Ergodic Theory and Dynamical Systems" (A. Katok, Ed.), pp. 211–333, Birkhäuser, Basel, 1981.
6. J. LLIBRE AND C. SIMÓ, Oscillatory solutions in the planar restricted three-body problem, *Math. Ann.* **248** (1980), 153–184.
7. J. LLIBRE AND C. SIMÓ, Some homoclinic phenomena in the three-body problem, *J. Differential Equations* **37** (1980), 444–465.
8. L. G. LUKJANOV, A study of asymptotic solutions in the vicinity of the collinear libration points of the restricted three-body problem, *Celestial Mech.* **15** (1977), 489–500.
9. R. P. MCGEHEE, "Some Homoclinic Orbits for the Restricted Three-Body Problem," Ph.D. thesis, University of Wisconsin (1969).
10. R. MARTINEZ, Moviments quasi-aleatoris en el problema restringit, circular i pla de 3 cossos, *Pub. Mat. Univ. Autònoma Barcelona* **24** (1981), 163–225.
11. J. MOSER, On the generalization of a theorem of Lyapunov, *Comm. Pure Appl. Math.* **11** (1958), 257–271.
12. J. MOSER, "Stable and Random Motions in Dynamical Systems," Princeton Univ. Press, Princeton, N.J., 1973.
13. K. A. SITNIKOV, The existence of oscillatory motions in the three-body problem, *Soviet Phys. Dokl.* **5** (1961), 647–650.
14. S. SMALE, Diffeomorphisms with many periodic points, *in* "Differential and Combinatorial Topology" (S. S. Cairns, Ed.), pp. 63–80, Princeton Univ. Press, Princeton, N.J., 1965.
15. V. SZEBEHELY, "Theory of Orbits," Academic Press, New York/London, 1967.

Printed in Belgium